INTERNATIONAL JOURNAL OF HYDROGEN ENERGY 47 (2022) 30759–30787

Available online at www.sciencedirect.com

ScienceDirect

journal homepage: www.elsevier.com/locate/he

Zeolite and clay based catalysts for CO_2 reforming of methane to syngas: A review

Hambali Umar Hambali [a,*], *Aishah Abdul Jalil* [b,c], *Abdulrahman A. Abdulrasheed* [d], *Tan Ji Siang* [b], *Yahya Gambo* [e], *Ahmad Abulfathi Umar* [f]

[a] *Department of Chemical Engineering, Faculty of Engineering and Technology, University of Ilorin, P.M.B. 1515, Ilorin, Nigeria*

[b] *School of Chemical and Energy Engineering, Faculty of Engineering, Universiti Teknologi Malaysia, 81310, UTM Johor Bahru, Johor, Malaysia*

[c] *Centre of Hydrogen Energy, Institute of Future Energy, 81310, UTM Johor Bahru, Johor, Malaysia*

[d] *Department of Chemical Engineering, Abubakar Tafawa Balewa University, P.M.B. 0248, Bauchi, Nigeria*

[e] *Department of Chemical Engineering, King Fahd University of Petroleum and Minrerals, Dhahran, 31261, Saudi Arabia*

[f] *Department of Chemical Engineering, Faculty of Engineering, University of Malaya, Kuala Lumpur, 50603, Malaysia*

HIGHLIGHTS

- Zeolite and clay based catalysts for DRM are systematically reviewed.
- Restructuring of supports enhance interaction of catalyst components.
- Higher amount of CO_2 in feed favours pure syngas production and improve catalyst life span.
- An in-depth analysis on progress, challenges and prospects are presented.

GRAPHICAL ABSTRACT

ARTICLE INFO

Article history:
Received 30 September 2021
Received in revised form
2 December 2021
Accepted 23 December 2021
Available online 10 January 2022

Keywords:
Dry reforming of methane

ABSTRACT

The development of coke and heat resistant catalyst for dry reforming of methane (DRM) is the major bottleneck towards the industrialization and commercialization of the process. Zeolite-based and clay-based catalysts are promising candidates for DRM to produce syngas (CO and H_2). The abundance, low cost, excellent properties and environmentally friendly nature of these support materials are an added advantage. Herein, this review entails the recent advances in development of zeolite and clay-based catalysts for DRM. In addition, the review captured a discussion on emerging trends in engineered mesostructured DRM catalysts. Tailoring of their framework configuration, pore architecture, crystals morphology and incorporation of active phases have led to the discovery of novel, robust

* *Corresponding author.*
E-mail address: hambaliuh313@gmail.com (H.U. Hambali).
https://doi.org/10.1016/j.ijhydene.2021.12.214

Zeolite
Clay
Syngas
Process parameters
Optimization

and high-performance catalysts. Notably, advances recorded in the catalysts synthesis procedures and characterization methods were also highlighted and elaborately discussed. It is expected that this review provide a comprehensive roadmap in the quest for an economically and industrially potent catalyst for syngas production via DRM.

Introduction

The industrial revolution and rising living standards have prompted serious environmental issues. Emission of hazardous gases from anthropogenic activities such as combustion of fossil fuels for heat, electricity and transportation purposes need to be reduced in order to counteract changes in the global climatic conditions [1–3]. The utilization of greenhouse gases (CO_2 and CH_4) to produce syngas (CO and H_2) provides alternative way to impede the menace of global warming. Conversion of these greenhouse gases into value added products could be achieved through methane conversion processes such as partial oxidation, steam reforming and dry reforming of methane [4–9]. The suitability of any of these technologies is dependent on availability of feed materials and desirable products as summarised in Fig. 1. DRM (Eq. (1)) is considered the most suitable reforming process because it produces syngas (H_2:CO ratio of unity) mixture appropriate for Fischer-Tropsch synthesis [9,10]. The DRM process, which is less expensive than the currently used carbon capture and storage technologies, could be efficiently used to sequestrate CO_2 gases. The process was first studied by Fisher and Tropsch in the year 1928 [10,11], and offers advantages over existing industrial syngas production process from both economic and environmental viewpoint. DRM is an environmentally friendly route since it's a pathway which consumes two of the principal greenhouse gases; thus, providing a beneficial means for reducing the climate change menace [12,13].

The development of an efficient and robust DRM catalyst without compromising activity and stability remains a hurdle. Being a highly endothermic reaction, equilibrium conversion of reactants in DRM is attainable only at high temperatures mostly in the regions above 700 °C [10,14,15]. Despite the meaningful conversion of reactants attained at these temperatures, the DRM process is faced with severe carbon formation due to the large fraction of carbon molecules in the feed gas and high reaction temperature. Moreover, propagation of methane cracking (Eq. (3)) and Boudouard reaction (Eq. (2)) increases the propensity of carbon deposition. The presence of reverse water gas shift reaction (Eq. (4)) induces higher stoichiometric conversion of CO_2 than CH_4 [5,16,17].

$$CH_4 + CO_2 \rightleftharpoons 2CO + 2H_2,\ \Delta H^0_{298K} = 260.5\ \text{kJ/mol} \quad (1)$$

$$2CO \rightarrow CO_2 + C,\ \Delta H^0_{298K} = -173.0\ \text{kJ/mol} \quad (2)$$

$$CH_4 \rightarrow 2H_2 + C,\ \Delta H^0_{298K} = 75.0\ \text{kJ/mol} \quad (3)$$

$$CO_2 + H_2 \rightarrow CO + H_2O,\ \Delta H^0_{298K} = 41.0\ \text{kJ/mol} \quad (4)$$

Remarkable DRM performance were obtained over kinds of noble metal based catalysts (Rh, Ru, Pt, Pd and Ir) [5,18,19]. Nonetheless, their application is not profitable and sustainable from an industrial standpoint. More so, noble metals are likely vulnerable to sintering at high temperature. As an alternative to the scarce and exorbitant noble metal catalysts, Ni-based catalysts have been the most widely tested. Nickel is relatively abundant with moderate cost and has an activity competitive with those of noble metals [18,20,21]. The demerit of nickel metal catalysts is their characteristic swift deactivation induced by carbon deposition and sintering. It is

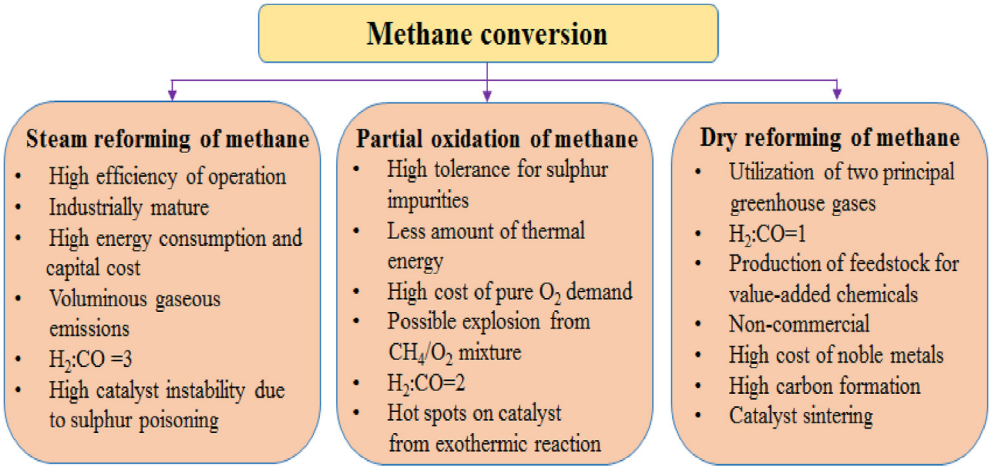

Fig. 1 – The scheme of methane conversion processes.

worthy of note that the effect of the carbon type, and mechanism of formation during DRM is still much debated and subject of continuous studies in academia. Despite the research successes recorded over recent years in catalyst development with remarkable activity and stability, the quest for novel and economically potent Ni catalysts with enhanced properties and performances is still much desired towards successful commercialization of syngas production via DRM.

A DRM pilot plant has recently been constructed by Linde group in Germany, which was aimed at determining the commercial readiness of DRM technology. The pilot plant uses Ni-based and Co-based catalysts. The plant performance test provided data on longer-term and complex process parameters, which pave way for investigation of optimization approaches towards development of a more broadly applicable process [10,22]. The successfully developed pilot plants are the CALCOR and SPRAG process [22,23]. The CALCOR process is only suitable for small-scale operation, with production of CO rich syngas (H_2:CO = 0.43). The SPRAG process was designed to combine the characteristics of DRM and SRM process. However, sulphur poisoning reduces the overall activity of the catalyst [10,24]. The state of the art DRM technologies seems feasible only in certain scenarios and lack breadth in applicability. Therefore, commercialization of DRM process is hinged on development of an economically potent catalyst with the required activity, stability and ease of regeneration.

Zeolites [25–29] are crystalline microporous aluminosilicates materials with high surface acidity, which have been explored as metal support. Zeolite have a porous crystalline framework, composed of tetrahedral SiO_4 and AlO_4 with oxygen atom as the interconnecting bridge between tetrahedra. Zeolites have been extensively used in acid-catalysed reactions and as catalysts support material for base reactions due to their well define pore structure, universal availability, high affinity for CO_2 as adsorbent, surface acidity, high surface area and intralattice pore volumes [3,29,30]. However, they usually contain varying levels of hydration, which leads to structural collapse due to harsh DRM conditions. Their surfaces contains high concentration of acid sites which often lead to side reactions with inferior stability [20,31,32]. Unprecedented research has been devoted over the years to fine tune porosity and surface acidity for better active metal dispersion and thermal resistance via approaches such as addition of promoters, dealumination and altering Si/Al ratio.

Clays [33–35] are abundant earthy materials which predominantly comprises of tetrahedral $[SiO_4]^{4-}$ and octahedral $[AlO_3(OH)_3]^{6-}$ layers. Clay materials have been considered as carrier materials for fabrication of DRM catalysts because of their remarkable attributes such as low-cost, abundance and peculiar structures and properties [35,36]. However, despite the economic benefits of clay material, their application is hampered as a result of less accessibility of reactants to active metal sites due to their intercrystalline mass transfer hindrance, thus, leading to particle agglomeration under the harsh DRM reaction conditions.

Several reviews have been produced which focus on catalyst design [9,14], influence of process parameters [21], model systems [10], development of nickel based catalysts [37,38], nanosilica-based catalysts [39], core-shell structured catalysts [40] and perovskite catalysts [41]. This review focuses on advancements in development of zeolite and clay catalysts for DRM. The fundamental aspects of zeolite and clay supports in DRM has not been specifically reviewed in literature, so it is right time to provide one. The review is organized as follows. Introduction of the general aspects of greenhouse gases emissions and mitigation with emphasis on CO_2 and methane utilization. This is followed by the main advantages and disadvantages of zeolite and clay supports in DRM. Emerging trends in fabricating structured support materials was also discussed. Thereafter, the impact of process parameters was discussed with emphasis on optimization of DRM process parameters. Furthermore, we also discussed about the emerging supported catalysts studied in DRM. The final section provides summary and conclusion of the review with outlook on the future of zeolite and clay based catalysts in production of syngas from DRM.

Greenhouse gases emissions and mitigation

The menace of climate change due to excessive release of greenhouse gases (GHG) remains an intractable problem. The GHGs (CO_2, H_2O vapour, NO_x and CH_4) emitted from anthropogenic activities such as combustion of fossil fuels for heat, electricity and transportation purposes have been established to be responsible for the menace of global warming [33,42–44]. The movement restrictions induced by the COVID-19 pandemic have slightly reduced industrial activities, which could reduce global energy demand and emissions. Nonetheless, after adequate implementation of vaccine program, upsurge in energy demand is anticipated. Generally, beyond 85% of the total energy demand is being supported by combustion of fossil fuels. Nevertheless, the use of fossil fuels for energy generation continually pose threats to the ecosystems, economy and human health [20,45]. Congruently, efforts have been made to address climate change mitigation as resolved in the Paris agreement (2015). The agreement is aimed at limiting the world's average temperature rise (below 2 °C) [32,46]. Along with the rapid rise of global population, world's total energy demand has been growing significantly. The global energy demand is anticipated to increase by more than 40% by the year 2035 [45]. In turn, more fossil resources are used for energy generation, which further escalates the threat of global warming. To alleviate this issue, there is a need for efficient use of energy. The feasible measure to limit the menace of global warming is to utilize greenhouse gases to produce value added products, thus limiting the harm to humans and environment that is induced by excessive emission of GHGs.

CO_2 emission and utilization

Carbon dioxide (CO_2) is an odourless, colourless and incombustible gas with higher (60%) density than that of pure air. CO_2 is a non-polar gas comprised of carbon atom covalently doubly bonded to two oxygen atoms with a characteristic stretching vibrations and deformation around the carbon nucleus [32,47,48]. Basically, CO_2 is a primary GHG emitted from several human activities and natural sources. While

production and consumption of CO_2 is indispensable, its' skyrocketing concentration in atmosphere is accompanied by severe and long-term consequences [43,49]. Based on the literature, CO_2 has been considered a primary GHG owing to global warming potential and concentration in the atmosphere which has dramatically increased from 340 ppm in 1980 to 408 ppm in the year 2019 [43]. According to data released by IPCC (Intergovernmental Panel on Climate Change), anthropogenic CO_2 need to be reduced by 50% in order to curtail the soaring average global temperature by 2 °C by the target year 2050 [50,51]. In addition, the model developed by IEA (International Energy Agency) predicated that worldwide CO_2 emissions must be maintained below 15 gigatons per annum to keep global average temperature below 2 °C.

The carbon capture, utilization and storage (CCUS) approach is needed due to its potentials to contribute around 16% total CO_2 reduction by 2050. Besides, 14% reductions in cumulative CO_2 emission from 2015 to 2050 is also anticipated in comparison to the period of no action [52,53]. The reduction of CO_2 emissions into the atmosphere can be achieved either by carbon capture and sequestration (CCS) or carbon capture and utilization (CCU). The CCS technologies are aimed at capture and subsequent storage of large quantities of CO_2. However, issues ranging from technical, economic and political need to be addressed in order to pave way for the industrialization of CCS process. From economic point of view, implementation of CCS is totally non-profitable because it requires substantial capital investment for the capture, storage and transportation of CO_2 [10,54]. The major technical challenge encountered includes limited geological storage capacity and leakages of sequestered CO_2 from their storage site. Thus, a further escalation of transportation and injection costs [55]. CO_2 capture from industrial plants is achieved via three approaches: (i) pre-combustion, (ii) post-combustion or (iii) oxyfuel process. Among these approaches, post-combustion is the most viable for existing process plants without concerns over retrofitting [54,56]. The reduction of global carbon footprint via CCU have recently been implemented as an alternative to CCS technologies. This has attracted global attention because it transforms captured CO_2 waste into value-added products and curtails the menace of global climate change. Thus, implementation of CO_2 utilization processes will not only curb global warming challenge, but also provide an economic return.

Methane sources and conversion

Methane (CH_4) is the simplest and most abundant among all the hydrocarbons, where large quantity of it is emitted from different industrial sources [29,57,58]. Methane is the primary component of natural gas constituting about 70–90% by volume. Since methane is a pivotal component of the global energy portfolio, its conversion into higher value products have been on the rise. This is partly due to its low cost and suitability as fuel source with less carbon footprint and emissions. The natural gas resources include the under exploited natural gas reserves due to technical and/or economic reasons but have great geological potentials for exploitation in the foreseeable future [57,58]. This does not also include methane trapped in the form of crystalline hydrates in shale rocks, ocean continental slopes, and permafrost zones.

Despite the tremendous and wide availability, CH_4 usage as a source of energy is still underutilized. This can be attributed to the nature of CH_4 gas from sources which require further purification before application as fuel source. The constitutes of CO_2 from natural gas relatively depends on its origin, production feed stock and purity of the gas in the reserves. The content of a pure gas is 0.05–1.5% CO_2, while biogas contains 35–50% of CO_2. High CO_2 content and low calorific value limits its direct use as fuel [10]. Some reserves are forsaken because their content makes their exploitation unprofitable. As a result, diminishing but still considerable amount of CH_4 as natural gas is flared in many countries. A projected amount of nearly $100 \times 109\ m^3$ gas are flared annually, which is about 4% of the total production [57,59]. Another issue related with direct usage of CH_4 as fuel is its characteristic low volumetric energy density at ambient conditions. This has negatively influenced the extent of its application especially for transportation purposes. To bolster its density for prolonged application, CH_4 is stored as compressed natural gas or liquified natural gas at extreme high pressure or low temperature respectively [58,60].

Methane conversion is of great significance in the sustainable supply of energy, fuel products and important chemicals for present and future societies applications. The process of transformation of methane to fuel and valuable products is pivotal in the area of heterogenous catalysis in the 21st century. This is because of the poor reactive nature of CH_4 due to its stable nature and weak polarity [14,61,62]. As such, activation of methane is very challenging. The activation process occurs through homolytic cleavage of C–H bond and transfer of hydrogen (H_2) atom from CH_4 to the neighbouring radical. The challenge of CH_4 activation can only be overcome by use of aggressive reactants or elevated temperature. Direct industrial routes for CH_4 conversion to desired products is limited and practically elusive, while the indirect route is to some extent more technologically advanced [63–65].

Catalyst system for DRM

The catalyst is considered as a key factor in transformation of CH_4 and CO_2 to syngas. As such, design of a robust catalyst system to efficiently perform the process with limited carbon laydown remains a hurdle [21,39,40]. The rapid and massive deactivation of DRM catalysts especially nickel-based catalysts is a major obstacle towards its commercialization and industrialization for value added syngas production. The detailed information on catalyst components beneficial for DRM process could be referred in our previous review [9]. In Fig. 2, we summarise the desirable attributes of robust catalyst for methane reforming process. Fabrication of an economically viable catalyst system depends on the extent of interplay between the catalyst components.

Several efforts have been focused on modulating crucial catalytic properties of catalysts for DRM [14,66,67]. Nonetheless, catalyst deactivation remains a major hurdle towards development of catalyst system for large-scale methane

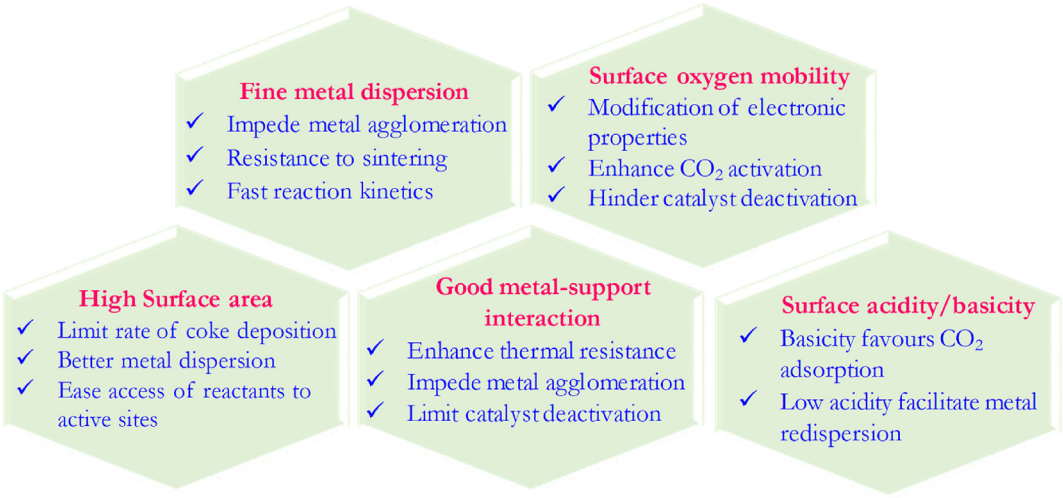

Fig. 2 – Schematic representation of crucial properties of robust catalyst system for DRM.

reforming process. Basically, catalyst lifetime is influenced by several factors including: pore structure [39,67], surface acidity/basicity [29,68], metal sintering [69], metal support interaction [40], crystal size of catalyst [1,19] and nature of feed [37,62,70]. For a DRM catalyst to remain active, variety of carbon forming reactions must be supressed. The main carbon forming reactions are Boudouard reaction (Eq. (2)) and methane decomposition (Eq. (3)). A higher rate of carbon formation occurs at higher temperatures, as a result of higher rate of methane decomposition than Boudouard reaction above 700 °C [9,37,71]. When these rates are balanced with carbon removal rate, carbon deposition on catalyst occur and can significantly affect catalytic performance. Several types of carbon could be formed, mostly termed as coke when formed by decomposition of long-chain hydrocarbon and carbon when formed via Boudouard reaction (nonetheless the two words are mostly used interchangeably) [37,69].

Basically, surface carbon formed during DRM can be classified as active or inactive carbon. Active carbon is formed via CH_4 dissociation as detailed in literature [1,10]. The formed inactive carbon species are deposited on catalyst surface via (1) continuous accumulation of filamentous or nanotubes carbon when carbon diffuses through active metal particle to the point that the particle is push away from the support, (2) encapsulation of active metal particle thus deactivating them completely, (3) physical adsorption in multilayers impeding diffusion of reactants to active metal sites [9,14,32]. Carbon formation and removal reactions on catalyst surface are illustrated in Fig. 3. When CO interacts with active metal sites it dissociates to produce coke deposits on the catalyst surface. Likewise, coke formed via methane cracking and homogeneous catalytic methane cracking reactions. Effective removal of surface adsorbed carbon species can be achieved via reactions such as carbon gasification with H_2O, methanization and reverse Boudouard reaction. These reactions are exergonic in nature and thermodynamically effective modes of carbon removal [70,72,73]. It was reported that existence of H_2O in the feed facilitates gasification of formed carbonaceous deposits on catalyst [70]. This is in line with the fact that addition of H_2O to DRM feed inhibit coke precursor formation. Takenaka et al. [74] affirmed that reverse Boudouard reaction is efficient for removal of coke deposits on Ni based catalysts. Schulz et al. [73] reported that high gasification rate of carbon species was achieved via methanization. Furthermore, it was discovered that feed composition significantly influences the amount and morphology of accumulated carbon [68,75].

Zeolite supported metal catalysts for DRM

Catalyst support is a material to which a catalyst is affixed. The support provides textural and physicochemical properties that is crucial in retaining active species dispersion and stability at harsh reaction conditions. The nature of the support significantly influences activity, selectivity, and stability of metal particles [32,37,67]. For practical and large-scale applications, thermal sintering and severe carbon deposition remains a bottleneck for Ni-based catalysts in DRM process. It has been demonstrated in literature that beneficial interaction between metal species and catalyst support is pivotal towards improvement of activity and impediment of catalyst deactivation by carbon deposition and high temperature metal sintering [15,39]. The nature of support material plays an integral role during initiation, adsorption and activation steps. CH_4 molecules are activated on active metal sites, and CO_2 activation occurs on either a basic or acidic support via bifunctional mechanism. Catalysts supported on inert silica support follow a mono-functional process, with reactants activation occurring on the metal surface [9,61]. Generally, strong interaction between catalyst components boosts dispersion of metal species to retain its small particle size at harsh DRM condition [14,62]. The stronger the metal-support interaction, the lower the tendency of metal agglomeration. Weaker metal interaction makes it beneficial for inert support catalyst system. This is because it was reported that weak interaction of metal and inert support material provides better metal-metal interaction [32,76]. Thus, the key to optimizing resistance towards catalyst coking and sintering is

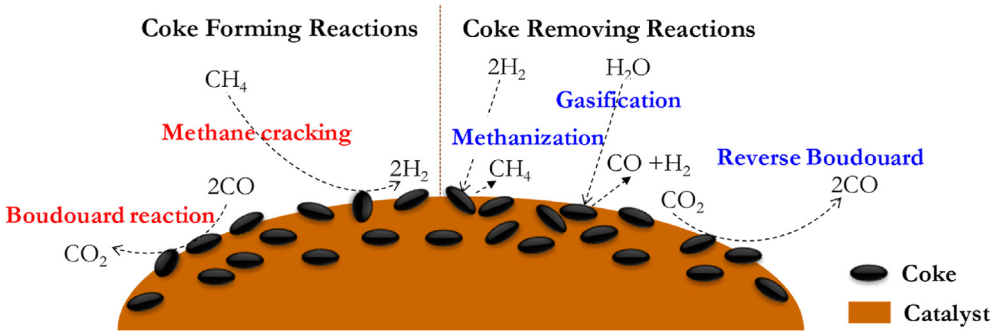

Fig. 3 – Carbon forming and removing reactions under CO_2 reforming of methane conditions. Reproduced from Ref.Wittich et al. [10] with permission from Chem Cat Chem, Copyright © 2020.

significantly reliant on rational design of support. Several investigations were conducted to address these hindrances, several of which are conclusively described in some literature [31,39,51,80].

Zeolites are crystalline microporous aluminosilicates materials with high surface acidity, which have been explored as metal support. They have a porous crystalline framework, composed of tetrahedral SiO_4 and AlO_4 with oxygen atom as the interconnecting bridge between tetrahedra [25,29,31,78]. The detailed information of zeolite structure could be referred in literature [25]. The acid sites are categorized as either Brønsted acid sites (BAS) or Lewis acid sites (LAS). The BAS is, by definition, a proton donor and is also known as protonic acid site, which usually exists in the form of a hydroxyl group. The LAS is an electron pair acceptor and usually appears as an unsaturated metal. The addition of metal cations can affect the surface acidity of zeolite, which leads to formation of new type of sites [29,30,79,80]. Adding metals can reduce BAS concentration while simultaneously creating new LAS, especially when the deposited metal atoms can exchange with zeolite sites.

Zeolite catalysts have gain significant attention over the years, especially in petroleum refining and petrochemical processes. It has been reported that worldwide zeolite consumption is around 275 thousand tons yearly [25]. Their activities are associated with their well define pore structure, plentiful supply, high surface areas, intralattice pore volumes, strong affinity for CO_2 as adsorbents and tunable active sites. Zeolite based catalysts have been studied for DRM [21,81]. However, zeolite contains varying levels of hydration, which led to structural collapse due to harsh DRM conditions [31,82,83]. Their surface contains high concentration of acid sites which often lead to side reactions with inferior stability. Furthermore, zeolite supported Ni catalyst suffers from rapid deactivation, which was associated with severe deposition of coke species in the cage of catalyst. This behavior was attributed to its microporous nature, which pose a threat to its application in practical and industrial scale operations [31,69,82,83]. Thus, accessibility of reactant/reaction products to active sites remain a challenging issue associated with conventional zeolite materials. As such, incessant research has been dedicated to modifying the textural, structural and chemical properties of zeolite support. Approaches such as use of surfactants, dealumination, addition of promoters, introduction of seed materials, altering pore volume and Si/Al ratio were explored [21,29,84]. Mesostructured zeolite support has enhanced pore size (diameter ranging between 2 and 50 nm) as compared to commercial zeolite support (<2 nm of diameter) [85]. Fig. 4 displayed a typical structure difference in terms of accessibility between the conventional microporous and hierarchical zeolite catalysts.

Zeolites such as silicalite-1, Y, Beta and ZSM-5 have been investigated as carriers for active metals [69,83,86]. However, ZSM-5 is among the most explored compared to other zeolites. ZSM-5 is a type of zeolite support with MFI (Mordenite Framework Inverted) structure. It was first synthesized by Argauer and Landolt in 1978 and patented by Exxon-Mobil [87,88]. It incorporates two channel systems comprising of a straight channel (5.4 × 5.6 Å), which is parallel with y-axis, and a sinusoidal channel (5.5 × 5.1 Å) which is parallel with x-axis. More so, it consists of a 10-membered ring with two distinct sets of intersecting channels. Thus, researchers consider ZSM-5 support as a good candidate for DRM catalysts.

Literature have shown that Ni-based supported ZSM-5 catalysts exhibit promising attributes for CO_2 reforming of methane reaction as presented in Table 1. It was found that performance of zeolite supported Ni catalysts depended simultaneously on morphology, reducibility, and acidity. Wei et al. [89] synthesized silicon carbide (SiC) coated on zeolite via hydrothermal synthesis method. The produced honeycomb-like catalyst (Ni/S-1/SiC) displayed improved catalytic activity and longevity during DRM. Hao et al. [90] prepared Ni/Al_2O_3 catalyst via sol gel technique. High surface area, ultrafine dispersed Ni crystallites and cooperatively interacting catalyst components were obtained, which produced excellence DRM

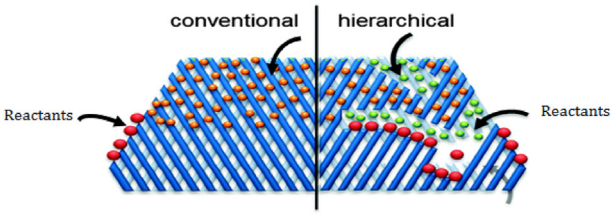

Fig. 4 – Structure improvement of zeolite designed at the hierarchical scale. Reproduced from Ref. Ennaert et al. [98] with permission from the Royal Society of Chemistry.

Table 1 – Zeolite based catalysts for CO_2 reforming of methane reaction.

Catalysts	Preparation method		Characteristics			Reaction temperature (°C)	CH_4 conversion (%)	CO_2 conversion (%)	TOS (h)	Carbon deposits (%)	Ref.
	Support synthesis	Metal loading	BET surface area (m^2/g)	Pore volume	H_2 consumption (mmol H_2/g)						
Pt@Silicalite-1	Microemulsion	Metal coating	362	–	–	670	57.2	68.3	12	–	[31]
Ni/ZSM-5	Hydrothermal	Colloidal dispersion	216.7	0.43 cm^3/g	–	800	96.2	–	–	–	[82]
Ni/ZSM-5	–	Ultrasound assisted dispersion	239	–	–	850	82	80	24	–	[113]
Ni-MCM-41	Hydrothermal	Wet impregnation	489	0.50 mL/g	–	750	~72.8	–	30	29.7	[175]
Ni-MCM(Al)-41	One-pot	–	1021	0.79 mL/g	–	800	~70	–	–	–	[112]
Ca–Ni/Y zeolite	–	Incipient wet impregnation	641	0.43 mL/g	–	700	59.4	66.1	5	25	[176]
Ni/H-ZSM-5	–	Incipient wetness impregnation	–	–	–	700	78.2	86.3	9	3.3	[177]
Ni/MFI	Microemulsion	Wetness impregnation	413	0.58 mL/g	–	800	69.85	72.4	30	–	[68]
Ni–Pt/Silicalite	Clear solution	Incipient wet impregnation	430	0.94 mL/g	–	800	~78.2	~84.6	20	1.0	[116]
Ni-MCM-41	Co-condensation	Solid-state grinding	706.8	0.7 mL/g	–	700	~78.9	~85	100	38.8	[106]
Rh–Ni/BEA	Sol-gel	Incipient wet impregnation	409	0.381 cc/g	–	700	74.4	77.4	7	2.85	[114]
Ni/ITQ-6	Sol-gel	Incipient wetness impregnation	350	0.15 cc/g	–	700	77	90	10	2.1	[109]
Ni/MgO-Beta	–	Incipient wetness impregnation	–	–	–	800	95	97	7	–	[178]
Ni–Mn/NH_4–Y	–	Wet impregnation	403	0.01 mL/g	–	700	49.6	52.4	24	–	[179]
Ni/ZSM-5	–	Dry impregnation	120	4.85 mL/g	–	800	~93	~97.2	30	12.0	[180]
Ni/Silicalite-1	Hydrothermal	Incipient wetness impregnation	300	–	–	700	77	84	10	4.0	[181]
Ni–MFI	–	Impregnation	332	0.22 cm^3/g	–	750	64	72	12	–	[182]
Ni–Co/ZSM-5	–	Wet impregnation	284	–	–	700	~62.8	~76.3	12	25.6	[81]
Ni–Zn-Silicalite-1	Microwave-assisted hydrothermal	Incipient wet impregnation	394	0.20 mL/g	–	750	84.5	75.4	12	38.3	[69]
Ni–Ce/ZSM-5	–	Incipient wetness impregnation	335.2	–	–	800	97.11	91.41	24	–	[100]
Ni–Mg/HY zeolite	–	Co-impregnation	352.7	0.43 cm^3/g	–	700	80.2	78.6	21	–	[101]
Ni/KH zeolite	Sol-gel	Impregnation	–	–	–	700	~91	~84.6	5	3.82	[183]
Co/zeolite Y	–	Sono chemical irradiation	262.7	–	–	850	79	88	10	–	[83]

performance. Apart from single-modal supported catalysts, bi-modal mesoporous supports have received recent attention due to their high accessibility and large surface area. The macropores facilitates diffusion of reactants and products, while the mesopores was responsible for microscopic dispersion of active species on the catalyst. Li et al. [91] reported a bimodal silica supported catalyst with Ni diameter of 3 nm using one-pot method, which produced significant DRM performance. More recently, bimodal alumina support comprising of mesoporous and macroporous was synthesized as summarised by Ma et al. [50]. The TEM analysis revealed the presence of ordered mesopores along with existing macropores. The bimodal support hindered graphitic carbon formation due to embedment of Ni particles into the mesoporous channels. Amin et al. [92] fabricated a trimodal porous silica using P123 and 1,3,5-trimethylbenzene as copolymer and swelling agent respectively. The presence of large pores induced higher accessibility resulting in improved DRM performance. More recently, trimodal hydroxyapatite structured supports have been developed as a potential DRM support due to their peculiar attributes such as thermal stability and less affinity to RWGS during DRM [93]. Therefore, the various structured supports focus on fabrication of an archetypical potent DRM catalysts.

Catalyst deactivation remains a major hurdle towards development of catalyst system for large-scale methane reforming process. Surface acidity or basicity is an indispensable parameter in designing catalysts which has been reported to significantly influence DRM process [61,68,94]. The acid and basic properties of catalysts system are extremely relevant for DRM, as they contribute to the propagation or impediment of coke forming reactions. Acidity of catalyst inhibit CO_2 adsorption onto catalyst support due to accretion of dehydrogenated carbon deposits leading to ageing and polymerization of carbon deposits rendering the catalyst inactive. Build-up of these inactive carbon species result in pore width shrinkage and active sites blockage leading to rapid catalyst activity loss [10,15]. However, catalyst basicity enhances adsorption of CO_2 which prevents growth and encapsulation of formed carbon species during DRM. The chemisorbed CO_2 is activated on the support material and active metal particle to produce carbonate intermediates which upon interaction with CH_4 molecules to produce CO [14,32,95]. Huang et al. [96] reported that the ability of coking resistivity is correlated with the strength and amount of basic properties of catalyst system as illustrated in Fig. 5. Affinity of acidic CO_2 molecules to catalyst surface is impelled by its basicity, thus improving CO_2 surface coverage and suppression of Boudouard reaction leading to carbon deposition.

Das et al. [61] scrutinized the impact of acidic/basic sites of SiO_2 and Al_2O_3 supported Ni catalysts in DRM. The authors found out that high acidity is pivotal in accumulation of carbon deposits due to oxidation of metal particles and occurrence of reverse water gas shift reaction (RWGS) reaction. To moderate acidity of catalyst systems, several promoting metals have been incorporated to the catalyst structure to enhance surface basicity. Alipour et al. [97] reported that basic promoters (MgO, BaO and CaO) supported on Al_2O_3 moderates basicity of Ni catalyst. Similar observations were reported in literature [10,98]. Ni et al. [99] investigated the impact of density and acidity/basicity of surface OH groups on Ni/Al_2O_3 catalyst by establishing a relationship between addition of B_2O_3 with carbon formation. Their findings revealed that introduction of 5 wt% B_2O_3 unto Ni/Al_2O_3 catalyst significantly suppress propagation of side reactions with inferior stability due to more basic OH groups. It was concluded that the higher the amount of these OH species, the higher the tendency of oxidation of CH species and carbon by basic OH species which lessen the chance of catalyst deactivation. Catalyst basicity have been demonstrated to improve DRM performance by lowering activation energy values of methane and carbon dioxide as discussed in our previous findings [16,48,68]. The activation barrier for carbon dioxide molecules is lower than for methane molecules due to less stable nature of the former than the latter. An interplay was found to exist between activation barrier and catalyst basicity. The basicity can be enhanced by utilization of basic support or promoter. Catalyst acidic/basic properties are contributed by one or a synergistic carrier material, active metal or promoter.

Metal promoted zeolite Ni catalysts for DRM

The focus of current researches is to find suitable support or promoter that will enhance catalytic performance, circumvent coke deposition and improve selectivity of target products. The rate and efficiency of DRM catalysts were found to be directly related to Ni surface structure. To counteract coking and deactivation of zeolite supported Ni catalyst, several promoters have been incorporated into the catalyst structure to improve interaction of catalyst components [16,48,68,81,100–103]. The summary of research findings

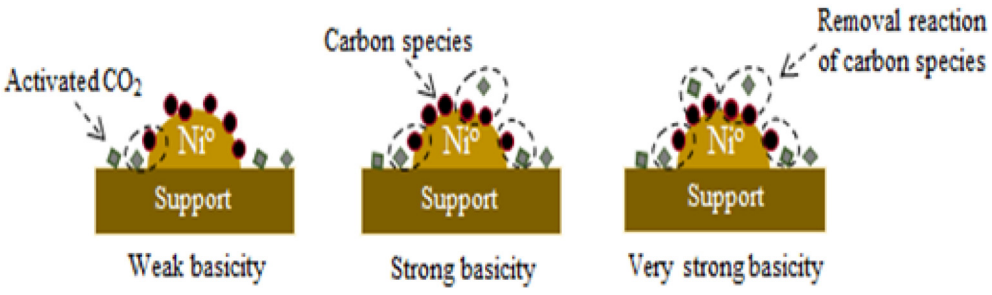

Fig. 5 – Conceptual model of the relationship between basicity and carbon removal on catalyst surface. Reproduced from Ref. Huang et al. [96] with permission from Elsevier.

utilizing various promoters to achieve better catalyst performance via different objectives to activity, stability and selectivity during DRM are presented in Table 1. The promoting metal could modify catalytic properties via bimetallic synergism, whereby the promoting metal may confer improvement in performance. Basically, promoting metals are classified as gasification or passivating metals. Passivating promoters such as Ag, K, Au and Sn could block the under-coordinated sites thereby hindering nucleation of carbon deposits on active metal sites [17,104]. Gasification promoters (Co, La, Ca, Ce) are typically introduced to accelerate oxidation of formed carbon species which result in swift gasification of the carbon species [16,17,39].

Estaphane et al. [81] conducted CO_2 reforming of methane reaction at GHSV 60,000 mL/g h over zeolite Ni catalysts. Following 12 h on stream at temperature of 700 °C, the cobalt promoted catalyst produced superior catalytic performance. The cobalt promoter acted as a synergist to Ni species supported unto ZSM-5, thereby improving DRM activity. Thermal analysis of spent samples revealed carbon within proximity of catalytic sites are responsible for deactivation, with the cobalt rich catalyst showing less carbon deposition. Introduction of Ce was reported to favor dispersion of Ni particles on ZSM-5 support which led to higher conversions and desired H_2:CO ratio [100]. The kinetic results also reveal 30% and 40% reduction in apparent activation energies of CH_4 and CO_2, which stem from the enhanced CO_2 chemisorption due to presence of Ce.

It was reported that introduction of CeO_2 into zeolite supported nickel catalyst suppresses high temperature sintering which enhanced catalytic stability [105]. The CeO_2 promoter induced generation of abundant basic sites, which facilitates adsorption and subsequent activation of carbon dioxide molecules on the catalyst surface. Enhanced CO_2 chemisorption increases CO_2 conversion thereby improving activity and selectivity for pure syngas (H_2:CO = 1) production. However, for development of cheaper catalyst, the exorbitant noble metal promoters are hardly considered in bimetallic Ni catalyst systems [10]. Conclusive report by our group [48] examined the role of several promoters (Mg, Ca, Ta, Ga) in enhancement of catalytic performance. The catalytic activity is in the order: Ni/ZSM-5 < Ni–Ga/ZSM-5 < Ni–Ca/ZSM-5 < Ni–Mg/ZSM-5 < Ni–Ta/ZSM-5. The reducibility of NiO on Ta promoted catalyst improved in the presence of Ta species, thus is responsible for an increase in catalytic activity. NH_3 and CO_2 TPD analysis revealed that the introduction of promoting metals altered the concentration of both acidity and basicity. It was found out that catalysts with high distribution of acidity or basicity were more susceptible to coking. As shown in Fig. 6, Ta promoted catalyst produced nearly stable CH_4 and CO_2 conversions throughout the 80 h TOS, which was ascribed to the unity acid/base ratio and improved interaction between components. Hence, a subtle interplay between acidity-basicity functions and metal-support interaction is pivotal to the development of zeolite support nickel catalysts.

Fabrication of robust zeolite catalyst for DRM

The method of catalysts synthesis has been established to control the structure of carrier material which consequently dictates the interaction that transpires. Several approaches have been adopted towards synthesis of efficient zeolite based catalyst with different degree of success. It was found that performance of zeolite supported Ni catalysts depended simultaneously on morphology, reducibility, and acidity. Bawah et al. [69] identified that high concentration of acidity on zeolite based catalysts propagates swift coke formation which induces deactivation. The smaller pore size of conventional zeolite support hinders penetration of metal species into the pore channels, which results in metal aggregation. Interesting findings by Zhang et al. [106] revealed the activity and stability of ordered mesoporous silica supported catalysts in DRM. The performance was in the order Ni-SBA-15 > Ni-KIT-6 > Ni-MCM-41. The porous bi-dimensional hexagonal structure of SBA-15 support resulted in strong interaction of catalyst components, thus, responsible for its remarkable carbon deposition. Similarly, when mesoporous supports, SBA-15 [96], MCM-41 [103], ZSM-5 [107] and MCM-22 [108] were tested in DRM reaction, Ni/SBA-15 exhibited higher CH_4 conversion (80%) in comparison to Ni/MCM-41 (52%) and Ni/MCM-22 (11%), whereas Ni/ZSM-5 the best conversion (96%) [82]. Higher surface area and better accessibility were major factors for the remarkable performance. $Ni/SiO_2–Al_2O_3$ also exhibited lower conversion compared to Ni/ZSM-5. Frontera et al. [109] studied the effect of various zeolite supported Ni catalysts and observed that the CH_4 conversion was in the order: Ni/Silicalite-1 (63%) < Ni/MCM-41 (75%) < Ni/ITQ-6 (80%). The better catalytic performance of Ni/ITQ-6 was correlated to stronger metal-support interaction and higher metal dispersion.

Catalyst fabrication via one-pot method is a strategic technique that involves subjection of multiple set of reactions and operations in a singular reactor. This is mostly executed in order to improve the chemical synthetic efficiency by minimising the number of steps, reduction of synthesis time and cost. The handling of toxic chemicals with the potential to cause harm is also minimised [29,110,111]. Reactions in this form of process is also referred as cascade, tandem or domino reaction to illustrate multi-step synthesis route taking place in one pot. Lovell et al. [112] prepared Ni-MCM(Al)-41 via one-pot technique. Incorporation of Al into the framework altered surface acidity which led to improved catalytic performance. The H_2-TPR and XRD results revealed the presence of highly structured, ultrafine dispersed nickel particles. Mesoporous structured supports (Ni-SBA-15, Ni-KIT-6 and Ni-MCM-41) have been synthesized via solid-state grinding technique and produced good performance in DRM. Vafien et al. [113] reported significant improvement of catalyst structure offered by employing ultrasound irradiation during preparation of mesoporous Ni/ZSM-5 catalyst. The dispersion of NiO on the ultrasound assisted Ni/ZSM-5 catalyst was studied by TEM analysis, where the size of nickel particles is below 100 nm, thus responsible in hindering carbon formation and increase in catalytic activity. Frontera et al. [114] reported post-synthesis treatment of silicalite-1 supports using hexamethyldisilazane (HMDS) as organo-silane. The abundance of silanol groups on the support surface during incorporation of nickel hindered nickel particles agglomeration, and favours nickel silicate species formation as schematized in Fig. 7. The organo-silane groups substituted the OH groups of the support

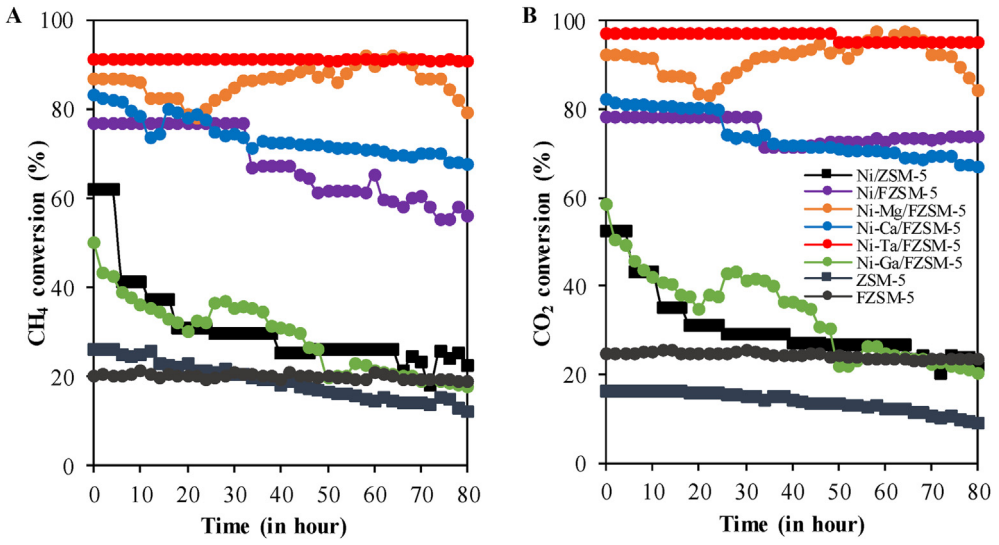

Fig. 6 – Time on stream performance of the catalysts. Reproduced from Ref. Hambali et al. [48] with permission from International Journal of Energy Research.

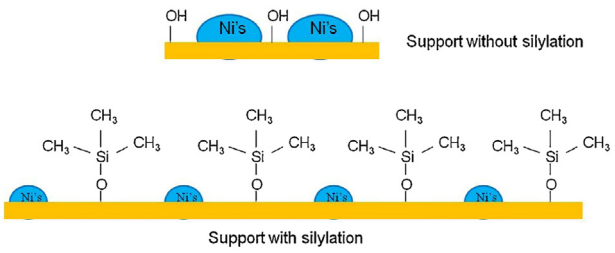

Fig. 7 – Proposed mechanism of Ni deposition on the silylated support surface. Reproduced from Ref. Frontera et al. [181] with permission from Elsevier.

leading to formation of ultrafine, more reducible Ni particles which not only enhance reactant conversion but also impeded coke deposition. More recently, it was reported that substitution of zeolite framework oxygen with nitrogen via nitridation process enhanced metal dispersion and basic properties [30]. Despite the weak basic nature of zeolite support, the inherent basicity was enhanced by nitridation at high temperature under flow of ammonia. The nitridation induce replacement of the framework oxygen species with nitrogen, which lead to formation of nitrided zeolite support with excellent DRM performance. As shown in Fig. 8, CO_2-TPD results showed that nitride ZSM-5 and beta catalysts had broader CO_2 desorption peak, signalling formation of more base sites as a result of framework nitrogen substitution. Basically, basic sites act as neutralizers to the acid sites thereby limiting occurrence of CH_4 dehydrogenation and enhance CO_2 chemisorption onto the catalyst surface, which boost carbon elimination via direct oxidation of deposited carbon to form CO [115]. The NH_3-TPD profile revealed decrease in strength of acid sites, which is advantageous to catalytic activity, because the acid sites promote coke forming side reactions [48]. Silicalite-1 support comprising of highly dispersed Ni–Pt nanoparticles was synthesized by clear solution method [116]. The TEM analysis revealed Ni encapsulated in hollow crystals which impeded coke formation. The hollow structured silicalite-1 support hindered carbon formed from affecting the activity of Ni particles inside the support, while the Pt additives led to better dispersion of metal nanoparticles. The encapsulation process improved corporative interaction between the support and metals (Ni and Pt), which was responsible for the coke and sinter resistant behavior during DRM process.

The technique of incorporation of metal species on support have also demonstrated crucial effect on overall catalytic performance. They positively affected the Ni crystallites by fine tuning its dispersion and interaction with the support structure [15,68]. Ensemble of studies reveal that appropriate impregnation method favor dispersion of active metals, impede crystallite migration and carbon deposition which could lessen the setbacks of Ni and Ni-based catalysts application during DRM. The widely employed impregnation methods in both industrial and academic research are wetness impregnation, incipient wetness impregnation, double-solvent, and physical mixing methods. Generally, water is the most considered solvent for dissolution of metallic precursor due to its high solubility [110]. The metal precursor is dissolved in a measured amount of water equivalent to pore volume of the intended support material. However, for the wetness impregnation method, the precursor solution is mixed in an excess solution, then drying to get rid of the excess solution. Irrespective of the method employed, the obtained solution is calcined at high temperature. In case of physical mixing methods, both metal precursor and support are physically mixed, with the resulting product heat treated in an inert atmosphere [68,117]. However, a contrary trend was recorded over Ni/MFI catalyst [68]. The physical mixing catalyst displayed drastic activity loss as a result of agglomeration of Ni particles. The wetness impregnation method is efficient to control the nature and interaction between support and active metals. Thus, the conventional impregnation methods could gain continuous relevance due

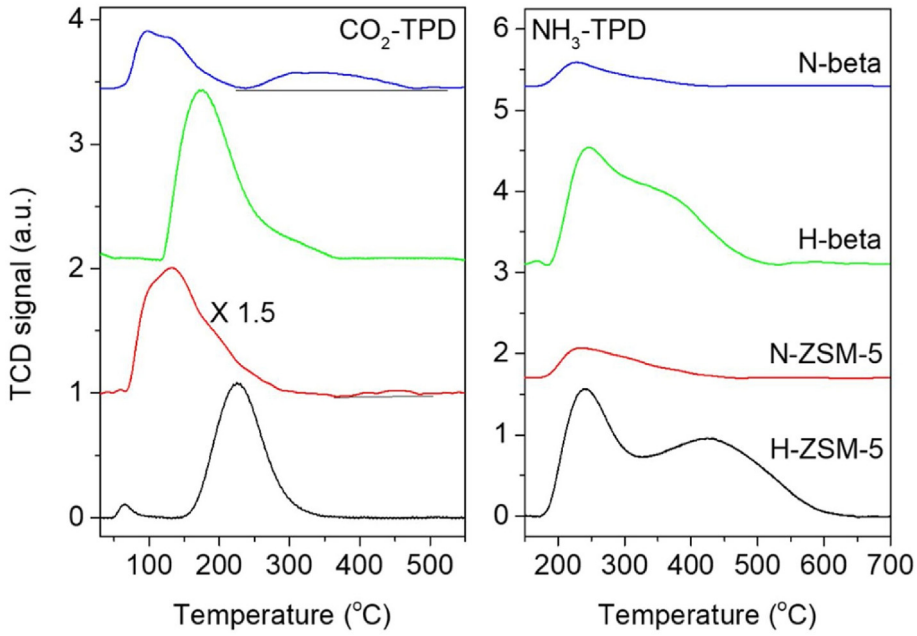

Fig. 8 – CO_2-TPD (left) and NH_3-TPD (right) profiles of H-ZSM-5, N-ZSM-5, H-beta, and N-beta zeolites. Reproduced from Ref. Kweon et al. [30] with permission from Elsevier.

to their simplicity, affordability, low waste production as well as ease in scale up.

Intrinsically, carbon laydown is inevitable during DRM as a result of the high reaction temperature [32]. According to our previous study [48], the coking behavior of Ta promoted catalyst was as a result of the nature and amount of carbon deposit. The rate determining step is methane dissociation, which occurs on the metal sites. As schematically revealed in Fig. 9, the DRM takes place by methane decomposition on the active metal sites producing CH_x species and H_2. Meanwhile, the liberated oxygen species via CO_2 activation oxidizes CH_x species to produce CO and H_2. The Ta promoted catalyst favored formation of O* species, which easily oxidise and eliminate surface carbon species formed. In the presence of Ta promoter, gasification of carbon becomes easier and less amount of coke are left on the spent Ni–Ta catalyst. Introduction of Ta metal induced immobilization of Ni sites which resulted in the superior performance. Contrastingly, the rate of reactants dissociation and carbon gasification is faster on Ta catalyst in contrast to unpromoted Ni/ZSM-5 catalyst. Hence, introduction of Ta changes the amount and nature of formed carbon species, which limited the tendency of agglomeration and coke formation.

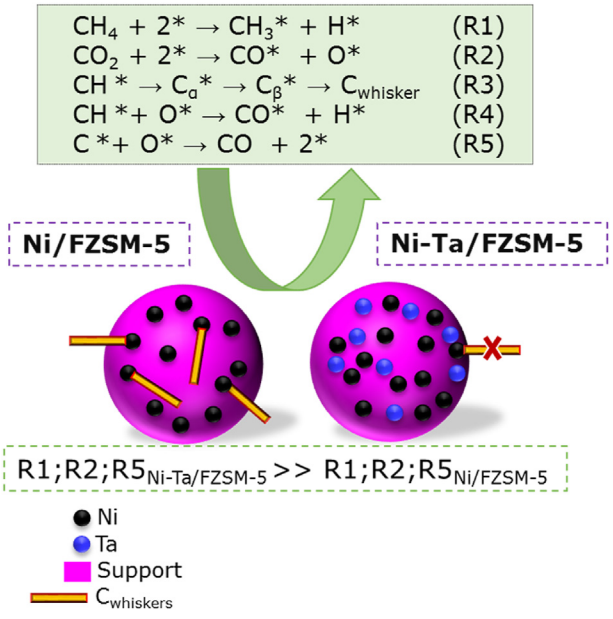

Fig. 9 – Reaction scheme for the dry reforming of methane over Ni/FZSM-5 and Ni–Ta/FZSM-5. Reproduced from Ref. Hambali et al. [62] with permission from Elsevier.

Clay supported metal catalysts for DRM

Clays are crystal structures which predominantly comprises of tetrahedral $[SiO_4]^{4-}$ and octahedral $[AlO_3(OH)_3]^{6-}$ layers. Clays are low-cost, microporous materials with unique structures and properties [34,35]. From an environmental viewpoint, clay materials are adjudged to be sustainable and green. Generally, clays are grouped as follows: (i) kaolinite comprising of clay materials such as kaolinite, serpentine and halloysite, (ii) 2:1 non-expanding which contains tetrahedral $[SiO_4]^{4-}$ and octahedral $[AlO_3(OH)_3]^{6-}$ in a 2:1 ratio (e.g., illite and mica), (iii) 2:1:1 group where an extra brucite octahedral layer is attached to a 2:1 mineral (such as chlorites), (iv) 2:1 group (limited expanding) comprising of vermiculite, (v) 2:1 group (strongly expanding) comprising of montmorillonite (vi) 2:1 group (uncharged) comprising of talc and pyrophyllite, and (vii) fibrous-layered silicates materials such as palygorskite

and sepiolite [34,118–121]. Out of the known clay materials, kaolin, is the widely reported to find application as highly stable catalyst support for DRM. Different physico-chemical attributes of these clay materials make them viable for DRM. These features include high surface area, micro porosity, small (nanoscale) sizes, layered structure, high adsorption capacity and high basicity.

Kaolin clays are among the most explored materials which comprises of a aluminosilicate with extremely crystalline hydrated layers in a 1:1 ratio of tetrahedron and octahedral [122,123]. Their surface area may extend to several square meters per gram and have been reported as support materials in various industrial applications owing to their unique physical and chemical properties. Kaolin clay contains varying amounts of oxides of alkali and alkaline earth metals (Na_2O, K_2O, CaO and MgO) which could serve as basic centers on support materials, thus favoring the CO_2 adsorption and activation [124]. Generally, kaolinite is the main mineral of kaolin, with others such as quartz and smectite. The raw kaolin is virtually inactive, thus the need for further treatments such as thermal, chemical or mechanical sequel to its application as catalyst carrier so as to provide the needed anchoring sites for the active metal species to avert a phenomena known as leaching [125–127]. Furthermore, migration of the active Ni nanoparticles into the support is a major issue associated with clay supported catalysts, which can be curtailed by appropriate Ni precursor preparation and incorporation. The most viable route is impregnation of the alumina material with Ni salts in aqueous solution, where the Ni^{2+} ions easily react with surface of an hydrated alumina thereby forming non easily reducible hydrotalcite phase after calcination [128]. Another common practice is organic functionalization through surface organometallic chemistry (SOMC) process which is effective in increasing selectivity of target products and deactivation resistance [129,130].

Kaolin supported nickel catalysts were investigated for the DRM under atmospheric pressure and reaction temperature of 700 °C [34]. The support was activated by acid or base in order to retain the kaolinite structure, while incorporation of metal precursor was achieved by organic ligand functionalized Ni synthesis protocol. The characterization results showed that the functionalized catalysts had small sized Ni particles with increased surface area for enhanced reduction and reaction. The XPS analysis shown in Fig. 10 revealed that functionalization of active nickel metal precursor with oxalate ligand hindered loss of Ni species during the synthesis process as supported by shifts of the peaks (Ni $2p_{3/2}$ and Ni $2p_{1/2}$) from lower to higher binding energies. The base treated functionalized catalyst produced the highest reaction rates for both reactants (CO_2 and CH_4) with yield of H_2 = 21.85% and CO = 28.49%. More so, it produced superior stability over the 20 h on stream DRM reaction. Similar observations were reported in previous studies [127,131,132]. The authors observed that deposition of the metal precursor using organometallic functionalization synthesis route produced nano-sized metal particles. The small Co/Ni nanoparticles with high dispersion and reducibility were responsible for the superior activities in contrast to others prepared via conventional routes.

The calcination and reduction temperature are also crucial parameters in determining the final morphology of clay

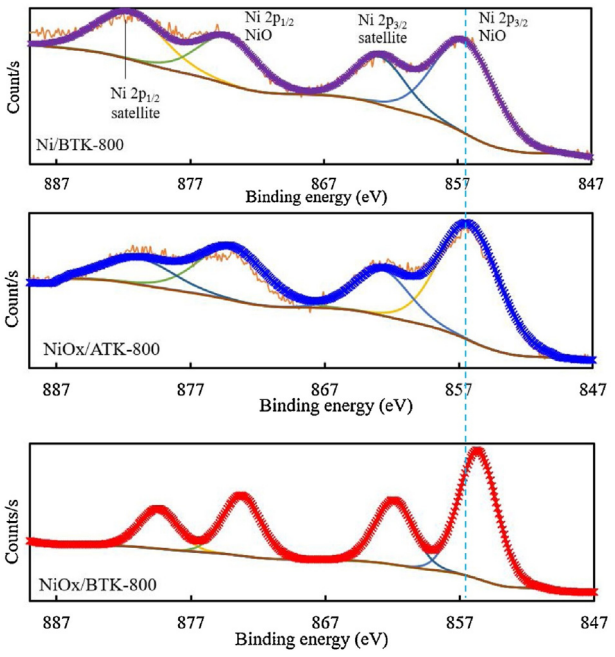

Fig. 10 – XPS Ni_{2p} scans of Ni/BTK-800, NiOx/ATK-800 and NiOx/BTK-800 catalysts. Reproduced from Ref. Ayodele & Abdullah [34] with permission from Elsevier.

supported catalysts. Usually, the activation method influences the size and dispersion of nanoparticles which in turn influence catalytic performance. Gamba et al. [133] reported that calcination temperature improved performance of Ni–Pr clay supported catalyst. The modified clay support was obtained in the presence of polyvinyl alcohol and microwave radiation, which led to the enhanced catalytic activity in contrast to unmodified counterpart. Thermogravimetric analysis revealed that calcination temperature had an impact on catalytic behavior, where catalysts calcined at 800 °C had null formation of coke in contrast to those calcined at 500 °C. Similarly, high catalytic stability and activity were reported in literature at 700–800 °C calcination temperature [130,134–136]. Baraka et al. [137] investigated the activity and stability of Ni-rich clay minerals sourced from natural lateritic ores deposit (Niquelandia, Brazil). Further study shows that the material composed of fraction of Fe (5.20 wt%) in the octahedral layers. The ore also comprise of tri-octahedral smectites with presence of Ni (23.8 wt%) within the octahedral sheets and Mg species (1.67 wt%) situated around the interlayer space. The raw Ni-rich clay minerals subjected to DRM process at low GHSV gave appreciable conversions (CH_4 = 49%, CO_2 = 63%) and stability. For the nickel rich samples, the performance improved signalling the positive influence of Ni species presence on both structural and exchangeable locations. TEM analysis of the spent catalysts (Fig. 11) showed presence of carbon nanotubes, situated around the Ni particles region for clay fraction reduced at 500 °C. The carbon nanotubes were not present in the case of catalyst reduced at 700 °C which corroborates its stable performance during DRM.

Basically, pre-treatment of catalyst prior to catalytic test plays a vital role in metal active sites formation, thus affecting catalytic performance. The catalytic activity of clay supported

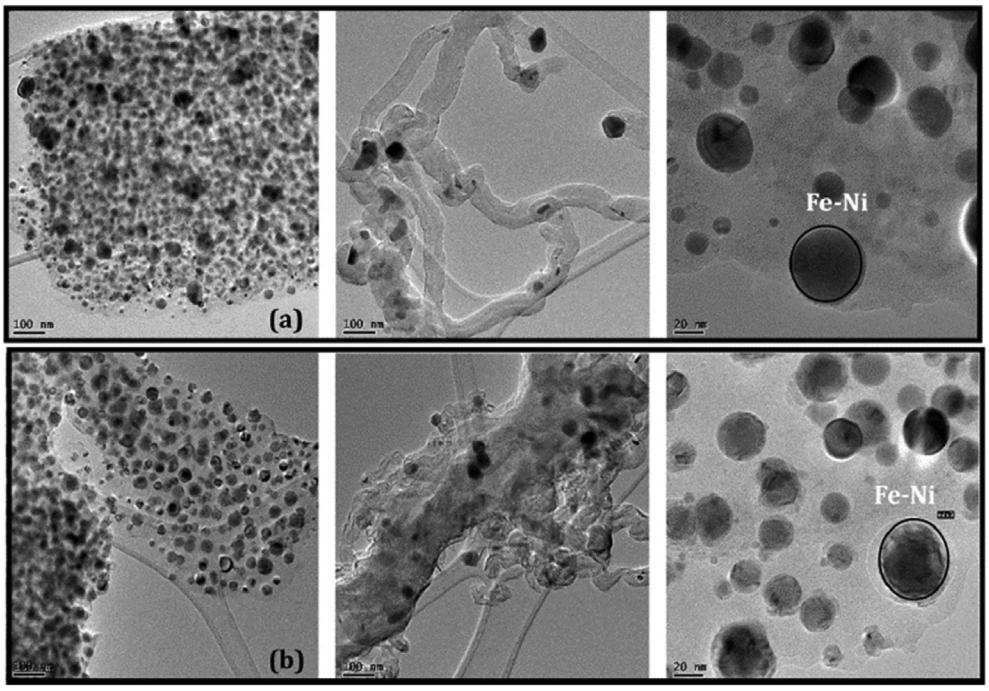

Fig. 11 – TEM images of for clay based catalyst after the DRM test pre-reduced (a) at 500 °C and (b) at 700 °C. Reproduced from Ref. Baraka et al. [137] with permission from Elsevier.

Ni catalysts modified by Fe or Cu were investigated in literature [138]. Carrying out the reduction temperature of 800 and 900 °C prior to the DRM reaction, the authors showed that reduction temperature had influence on basicity and Ni particle size. The catalysts reduced at 800 °C produced better catalytic performance in contrast to the ones reduced at 900 °C. This observations are in accordance with the literature findings [139,140]. Therefore, in order to achieve appreciable catalytic performance, it is important to apply appropriate calcination and reduction temperatures.

Liu et al. [43] explored the impact of various promoters (Al, Mn and La) on Fe-modified clay based catalysts as summarised in Table 2. The introduction of promoters altered the NiO crystallite size in the order: Ni–Al/Fe-clay (9.2 nm) < Ni–La/Fe-clay (9.8 nm) < Ni–Mn/Fe-clay (10.6 nm) < Ni/Fe-clay (13.4 nm). Their enhanced catalytic performance was correlated to the less strength of basic sites, enhanced dispersion and reducibility of Ni sites of Al/La promoted catalysts. On the other hand, Mn-promoted catalyst was least active due to strong Mn–Fe interaction and sintering. However, despite the good dispersion and reducibility of Mn-promoted catalyst, lower conversion of both reactants was observed. This can be correlated to the presence of fayalite and Mn rich sites, which could partially or completely cover the active Ni sites. Similar observations were reported in literature [141,142]. A highly stable Ni–Ce/Clay catalyst was synthesized by modification of the mineral clay with polyvinyl alcohol and microwaves radiation [143]. The catalyst is made up by open and rigid structures typical of mesoporous-type support. The stable performance was dependent on the structure of nickel sites and promotional species. The TGA analysis revealed negligible coke deposits on spent Ni–Ce/Clay catalyst.

The catalytic performance of Ni catalyst supported on Al–La pillared clay were examined by Wang et al. [144]. Carrying out the DRM reaction (at 1:1 feed ratio and 18,000 cm^3/h g), the authors showed that the incorporation of La enhanced the catalyst basicity; thus, influencing catalytic stability. The good performance of pillared clay was in good agreement with conclusions by Liu et al. [142]. The catalytic performance of Ni catalysts supported on zirconia pillared laponite clays with surfactants have been evaluated (GHSV = 18000 mL/g h) [90]. The amount of surfactant added in the preparation stage of

Table 2 – Physicochemical properties and catalytic performance of different promoter loaded Fe-clay catalysts in DRM reaction [43].

Catalysts	Metal Loadings (wt.%)	NiO crystal size (nm)		H_2 consumption (mmol H_2/g)	Surface area (m^2/g)	Pore volume (cm^3/g)	Total basicity (mmol CO_2/g)	Conversion (%)		Carbon deposits (mg)
		Reduced	Spent					CH_4	CO_2	
Ni/Fe-clay	Ni:15	13.4	–	2.03	44	0.11	22.58	17.8	22.1	109.4
Ni–Al/Fe-clay	Ni:15, Al:10	9.2	13.8	1.52	63	0.11	5.95	53.1	62.0	284.8
Ni–Mn/Fe-clay	Ni:15, Mn:10	10.6	12.6	2.28	45	0.15	19.44	2.5	1.4	15.1
Ni–La/Fe-clay	Ni:15, La:10	9.8	17.3	1.83	13	0.10	6.76	47.2	58.2	239.6

the modified clay catalysts were 4, 8 and 12 g. Ni/Zr-Laponite (8) gave the highest conversions (CO_2 = 95% and CH_4 = 85%) at reaction temperature of 750 °C. Moreover, N_2 adsorption conducted on the fresh and spent catalysts showed only minor decrease in porosity, signalling good metal-support interaction. Ni catalysts supported on alumina intercalated laponite clay prepared with polyethylene oxide surfactant have been examined in DRM reaction [145]. The authors reported conversions between 80 and 95% at reaction temperature of 800 °C. The surfactant tailored formation of a well-developed porous catalyst system with good dispersion of active species. In addition, Ni-containing phyllosilicate clay catalyst have been prepared via hydrothermal method [146]. Partial reduction of Ni species in thermally stable phyllosilicate led to better dispersed Ni nanoparticles, thus, inhibiting coke deposition during the methane reforming reaction.

Emerging trends in engineering mesostructured support

Catalyst deactivation remains a major hurdle towards development of catalyst system for large-scale methane reforming process. Regardless of the synthesis route or type of support material used, severe activity loss has been recorded during DRM especially over nickel catalysts. Ensemble efforts were aimed at understanding deactivation process models, fabrication of robust catalyst system and optimization for less carbon deposition. As discussed in the previous section, catalyst deactivation is induced from carbonaceous species formation and depositions, high temperature metal sintering and fracture of support. In view of the remarkable attributes of mesostructured catalyst systems in DRM reaction, more novel porous materials could also pave way for industrialization of DRM process. For example, materials such as core-shell, birdcage, york shell, fibrous among others can provide large surface area and fine metal dispersion which make them attractive candidates for CO_2 reforming of methane.

Confinement of metal particles inside shell structured support such as yolk-shell has proven to be a viable approach to prevent sintering of metal and carbon formation during DRM. This has triggered unprecedented research on design of spherical structured catalysts via modification of the synthesis route [86,147]. Several structured supports have effectively been applied in methane reforming reaction with positive impacts, especially the yolk-shell and core-shell configuration. Fabrication of core-shell support was attained via coating of metal nanoparticles inside large surface area support for better dispersion [91,92,148,149]. Encapsulation of metals particles inside core-shell support shields the active metals from coking, which hinder agglomeration of metal phase and subsequent deactivation. The spherical structure is achieved via an initial reaction to develop active metal seeds as the core, while the shell coating the core is produced from introduction of separate reactants [150].

Kawi and co-workers report the design of a yolk shell structured (Ni@SiO_2) catalyst by micro-emulsion method (Fig. 12) [151]. Excellent interaction between the metal core and the silica shell plays a vital role in enhancing activity and carbon resistance. The rational is to synthesize Ni catalysts which hinder growth of filamentous carbon species on catalyst surface during DRM reaction. It was reported that core-shell Ni@SiO_2 exhibited remarkable resistance to coking during reforming reaction as compared to commercial Ni catalyst [152]. The combination of micro-meso pores in the silica shell facilitated diffusion and hindered carbon filament growth. In this regard, core shell structured materials seem viable in commercial production of syngas by DRM process.

Fibrous material are another promising class of support material that was successful designed and for first time fabricated by the catalysis centre of King Abdullah University of Science and Technology, Thuwal [153]. The novel material was named KCC-1 (KAUST Catalysis Centre 1) with fibrous morphology as portrayed in Fig. 13. It offers high surface area as a result of dendrimeric silica fibers and their respective large pore channels, which enables better dispersion on the surface, thereby improving accessibility to active sites [154,155]. Microemulsion is a thermodynamically stable and optically isotropic solution that consist of water, oil, and amphiphilic molecule. The balance between these elements is crucial in dictating successful microemulsion formation. Exploitation of different surfactant result in different microemulsion formation, as a consequence of different packing parameter and interaction with oil-phase and aqueous-phase. Surfactants are compounds comprising of covalently bonded hydrophilic and hydrophobic parts. The hydrophobic part is called tail group, while the hydrophilic part is referred as head group. Increase in concentration of surfactant will intensify amount of adsorbed surfactant in the adsorbed layer until saturation is attained. Consequently, at the saturation point the surfactant dissolve in the aqueous phase, and the free energy of the system increases due to unfavourable interaction between hydrophilic groups with water. To aid minimization of free energy of the system, surfactant tends to form micelle via self-assembly process [156,157].

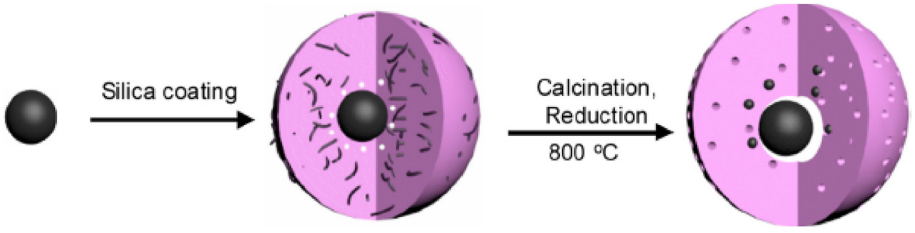

Fig. 12 – York-shell structure Ni@SiO_2 catalyst. Reproduced from Ref. Li et al. [151] with permission from American Chemical Society Catalysis.

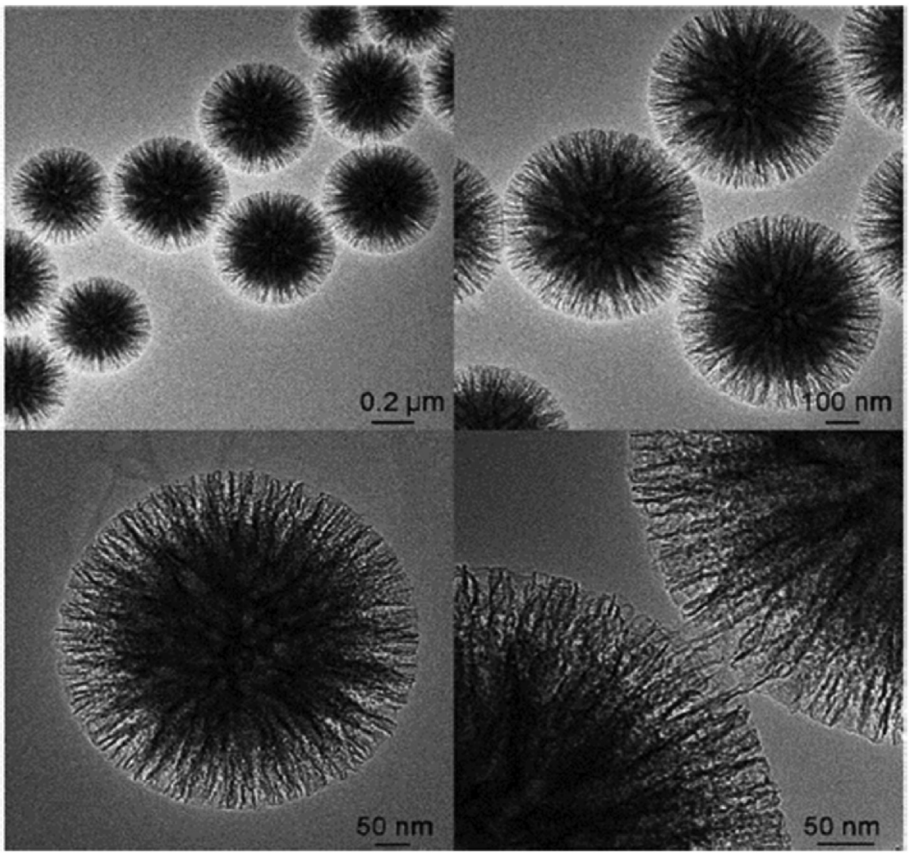

Fig. 13 – TEM images of KAUST Catalysis Centre 1 support. Reproduced from Ref. Polshettiwar et al. [153] with permission from Angewandte Chemie International Edition.

Basically, factors such as surfactant, oil phase, and aqueous phase play critical roles in formation of the fibrous morphology. Microemulsion system has been adapted in the development of zeolite materials. It was reported that microemulsion in zeolite synthesis act as confined space for zeolite growth [158]. Using non-ionic surfactant, addition of butanol as co-surfactant, and heptane as oil source. The utilization of water-in-oil microemulsion was reported to improve physiochemical properties of MFI structured silicalite-1 zeolite. Similarly, Maity & Polshettiwar [157] employed microemulsion synthesis technique for fabrication of fibrous structured nano materials.

Jalil et al. [84] reported the preparation protocol for fibrous zeolite Y as displayed in Fig. 14. The significant enlargement of intrinsic micropores of conventional zeolite Y was achieved via water-in-oil microemulsion method imposing dendrimer silica fibre growth on the zeolite support framework. The microemulsion system comprised of cetyltrimethylammonium bromide (CTAB) (as surfactant to direct structure growth), butanol (as co-surfactant), water (as aqueous phase) and toluene which act as the oil phase. After the addition of the zeolite Y seeds, coulombic attraction forces the CTA^+ species (hydrophilic head) into the zeolite Y pores. The zeolitic framework being negatively charged function as the nucleation center, with majority of the hydrophilic head generating reverse micelles round the hydrophobic tails targeted into the organic phase. The introduced Tetraethyl orthosilicate (TEOS) (act as silica precursor) hydrolyzes via interaction with the hydrophobic tail of the CTA^+ ions and aqueous phase into polar products. Finally, the produced paste is dried, calcined and filtered in order to drive off occluded and surface-located CTA^+ surfactant; thus, producing a fibrous structured support.

Fibrous ZSM-5 (FZSM-5) with high metal dispersion and stabilization tendency have emerged recently, which can improve mass transfer of reactants to the active sites and coking resistance [68,159]. FZSM-5 support possesses enhanced pore size (diameter ranging between 2 and 50 nm)

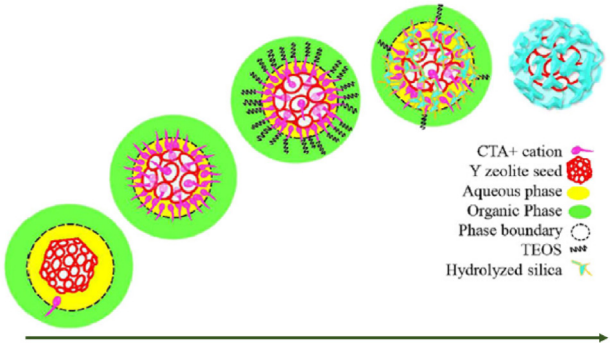

Fig. 14 – Schematic representation of fibrous zeolite Y synthesis. Reproduced from Ref. Jalil et al. [84] with permission from International Journal of Energy Research.

as compared to commercial ZSM-5 support (<2 nm of diameter). The FZSM-5 has a large surface area of (603 m^2/g) and pore volume (0.9704 mL/g), which upon undergoing DRM retained particle dispersion over long time on stream. The nature of carbon species on FZSM-5 supported catalyst are mostly amorphous in nature in contrast to the observed graphitic carbon on conventional ZSM-5 supported catalyst. Kobayashi et al. [31] revealed a new strategy to fabricate birdcage type Pt@Silicalite-1 zeolite catalyst. Typically, they used water-in-oil microemulsion technique to encapsulate the Pt nanoparticles unto the Birdcage structure as revealed in Fig. 15. They recorded a stable DRM performance at 620 °C over 24 h TOS. Recently, fibrous structured catalyst system produced excellent performances in carbon dioxide methanation [3,79,160–162], organic pollutant degradation [163–166], isomerization [84,167], methylation [26,27], methane reforming [71,77,162] and carbon dioxide capture [5,168]. Despite successes recorded over the years, development of novel mesostructured support with remarkable activity and stability is indispensable towards successful commercialization and industrialization of the process. Thus, engineering structured zeolite and clay can be a new source for perspective DRM catalyst supports with enhanced performance and thermal stability.

Role of DRM process parameters on catalytic performance

Several literatures on modulating catalyst properties for enhanced performance has been discussed in the previous sections. However, apart from the above measures employed in circumventing excessive coking, varying process parameters could be pivotal in controlling carbon resistance during the methane reforming reaction. As elaborated in previous studies [62,70,169,170], operating temperature of 700 °C favours the occurrence of DRM due to its exothermic nature. It was found out that thermodynamic driving force for carbon formation diminishes at higher temperature (>800 °C). Feed composition is another factor which plays a significant role in dictating the products spectrum and carbon deposition [73]. It was also observed that higher concentration of methane in the feed encourages catalyst deactivation. This indicates the propensity of carbon formation when composition of methane in the feed is high.

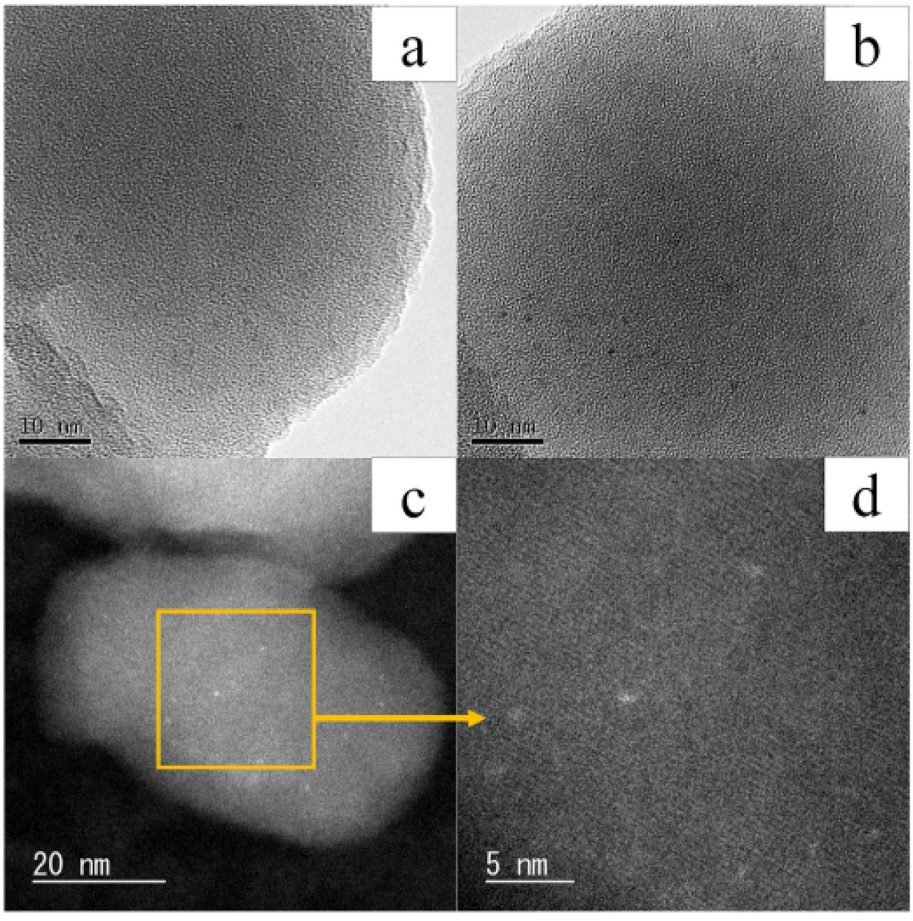

Fig. 15 – Images of synthesized Birdcage-type catalysts: (a) FE-TEM image of 0.1 wt% Pt@Silicalite-1, (b) FE-TEM image of 0.2 wt% Pt@Silicalite-1, (c) and (d) HAADF-TEM images of 0.1 wt% Pt@Silicalite-1. Reproduced from Ref. Kobayashi et al. [31] with permission from Elsevier.

Optimization of process parameters by response surface methodology

Response surface methodology (RSM) is an analytical technique to identify a suitable experimental design. It is also employed to improve and optimize complex processes that is achieved via mathematical and statistical techniques. Since the discovery of RSM by Box and Wilson in 1950s, it has been widely adopted in specific scenarios where numerous input parameters influence the performance of the process system [62,171,172]. The performance measurement parameter is known as the response or dependent variable, while independent variables are the input variables. The independent variables represent target variables that are manipulated by the engineer or scientist [17,169]. Basically, optimization using RSM take into cognisance multi-variate designs which involve the simultaneous combinations of factors that are likely to affect the outcome of a response.

The RSM is an advancement over the one factor at a time method which considers only a single factor at a time. Therefore, RSM technique typically involves development of experimental designs to explore the space of the independent variables. Also, it involves empirical statistical design models to describe an approximate relationship between response and input variables. In addition, RSM involves optimization design to determine the input variables that yield the desired and optimal value of the response. Basically, selection of design is imperative for optimization by RSM, since it specifies the experiments to be conducted in the experimental region of studies [62,173,174]. Some experimental matrices were conducted for this purpose. Factorial design is an example of experimental designs that are suitable for application on data set with no curvature. However, for experimental data that are not suitably described by linear functions, quadratic experimental design responses such as Box-Behnken, 3-level factorial and central composite designs are mostly considered. RSM tool can be found in computer-aided software such as Design Expert, Minitab and STATISTICA [36,173].

The RSM has over the years been used to conduct optimization of DRM process parameters. Table 3 is a summary of optimization studies of DRM process parameters using various catalyst configurations. It was found that central composite design (CCD) and Box-Behnken design (BBD) are widely adopted. The BBD interface is considered less expensive because it produces fewer experimental runs. The CCD is even more commonly used due to its vast usefulness in sequential experiments built on previous factorial experiments via addition of axial and centre points. Abdulrasheed et al. [17] reported the use of CCD interface to investigate the effects on GHSV, reaction temperature and CO_2:CH_4 ratio on methane conversion over Ni–La@KCC-1. The effect of temperature was observed to be profound on the DRM process. Hossain et al. [36] adopted CCD to investigate the effect of their variables on reactants conversion as well as yields of CO and H_2. To uncover the impact of elevated pressure on DRM process, study conducted by Izhab et al. [171] revealed that effect of gauge pressure on CO and H_2 production is significant. Concerning the response variables, CH_4 conversion is frequently considered as most suitable response in DRM. This results from the fact that the rate determining step in the methane reforming reaction is the C–H bond activation [11,14].

Existing DRM plants and patents

Obviously, most of the DRM research in literature was done in fixed bed reactors. As discussed in previous sections, DRM is an industrially immature process due to operational constraints displayed by the catalysts involved. Development of industrial DRM plants is generally at the nascent stage mostly at laboratory or pilot stage, and the reported plants are presented in Table 4. Several DRM patents are available on types of reactors for DRM process as elaborated in literature [21,195]. These include auto-thermal reactor [196], microwave reactor [197] and membrane reactor [198]. However, both fixed bed and fluidized bed reactors exhibit promising potentials, there commercial scale application remains a challenge. A detailed computational fluid dynamic (CFD) simulation could provide more information about various approach to improve performance of DRM reactors.

Recent supported catalysts studied in DRM

The present section aims to discuss recent advances related to supported DRM catalysts. Obviously, apart from zeolite and clays, other important materials have been extensively explored as supports in the development of DRM catalysts. The active phases are either in monometallic, bimetallic, or tri-metallic form, with nickel being the major active component. Metal oxides (MO) and mixed metal oxides (MMO) constitute an indispensable class of support materials in DRM. The oxides can be classified as reducible (CeO_2, TiO_2, and Fe_3O_4) or non-reducible (SiO_2, Al_2O_3, MgO, ZrO_2, and La_2O_3). Notably, the nature of support material can strongly influence the overall catalytic activity and selectivity of the supported DRM catalyst. Additionally, the choice of support coupled with the synthesis strategy deployed in stabilizing the active phase can affect the stability of DRM catalysts during TOS performance [203,204]. This is due to the fact that different supports have different physicochemical properties which could potentially account for significant variation in the interactions between the supports and the active phases. Such interaction is usually term as metal-support interaction, and it is an important lever to improve coke-resistance of several DRM catalysts [205]. Typically, Li et al. [206] reported the tuning of the metal-support interaction of CeO_2-supported Ni catalyst as an effective tool to control the catalytic activity and coke formation tendency via modulating the catalyst reduction temperature. The authors revealed that reduction of the Ni/CeO_2 at elevated temperatures ($\geq$873 K) promoted significant migration of ceria species from the reduced support to the active phase, prompting the partial encapsulation of the Ni nanoparticles and strongly stabilized them against severe agglomeration. Slight decline in activity of the catalyst was observed due to loss in the surface concentration of the Ni active species, however, the stability of the catalyst was significantly improved. Engineering abundant macropores on

Table 3 – Summary of research outputs on DRM optimization process.

Exp. design	Input variables	Response	Catalysts	Optimal process performance	Ref.
BBD	i. Feed ratio ii. CH_4 partial pressure iii. CO_2 partial pressure iv. Temperature	i. CO_2 conversions ii. CH_4 conversions	Co/CeO_2	Optimum feed ratio of 0.60 and CH_4 partial pressure of 46.85 kPa at 728 °C with CH_4 and CO_2 conversions of 74.84 and 76.49%.	[184]
CCD	i. Reaction temperature ii. CH_4:CO_2 ratio Gauge pressure iii. GHSV	i. H_2 yield ii. CO yield	Cobalt based	The optimum values of both responses (CO and H_2) corresponded to 903 °C, feed ratio of 1.31, GHSV of 4488 mL/h.g catalyst and 0.88 bar(g).	[171]
BBD	i. Ni content (wt%) ii. Cu content (wt%) iii. Temperature	i. CH_4 conversions ii. H_2/CO ratio iii. Deactivation	$Ni–Cu/Al_2O_3$	10 wt% of Ni, 0.83 wt% of Cu at 750 °C. CH_4 conversion of 95.1%, and deactivation of 1.4%.	[185]
CCD	i. Temperature ii. CO_2:CH_4 ratio iii. GHSV	CH_4 conversion	Ni–Ta/ZSM-5	Optimum CH_4 conversion of 96.6% at 784 °C with CO_2:CH_4 feed ratio of 2.52 and GHSV of 33,760 mL/g h.	[62]
BBD	i. Reaction temperature ii. CH_4/CO_2 ratio iii. O_2/CH_4 ratio	i. CO_2 conversion ii. CH_4 conversion	Commercial Ni Nano powder	82.9 and 90.8% of CH_4 and CO_2 conversions achieved at optimal reaction conditions of 900 °C, 1.5 of CH_4/CO_2 ratio and 0.10 ratio of O_2/CH_4.	[186]
CCD	i. Temperature ii. CO_2:CH_4 ratio iii. GHSV	i. CO_2 conversions ii. CH_4 conversions iii. H_2 yield iv. CO yield	$15Ni/CaFe_2O_4$	Reactants conversions (CH_4 = 85% and CO_2 = 88%) and yields (CO = 77.82%, H2 = 75.8%) achieved at optimal reaction conditions of 832.45 °C, feed ratio of 0.96 and 35,000 mL/g h.	[36]
CCD	i. La loading ii. Ni loading iii. Calcination temperature	CH_4 conversions	$La_{1-x}Ce_xNi_{1-y}Zn_yO_3$	Ni content effect is considerable and calcination temperature has a partial effect.	[187]
CCD	i. Temperature ii. Feed ratio iii. GHSV	i. CO_2 conversion ii. CH_4 conversion iii. H_2/CO ratio	10Ni/DFSAB-15	Reactants conversions (CO_2 = 95.67%, CH_4 = 93.48%) and H_2/CO ratio of 0.983 achieved at optimum conditions of reaction temperature 794.37 °C, feed ratio of 1.2 and GHSV of 23,815 mL/g h.	[19]
CCD	i. CO_2:CH_4 feed ratio ii. GHSV iii. Temperature	CH_4 conversions	Ni–Co/MSN	CH_4 conversion is 97% at reaction temperature of 783 °C, CO_2:CH_4 ratio of 3, and GHSV of 38,726 mL/g h.	[188]
CCD	i. Temperature ii. CH_4/CO_2 molar ratio	i. CO_2 conversion ii CH_4 conversion iii H_2/CO ratio	Ni/SiO_2	Reactants conversions (CO_2 = 83.1%, CH_4 = 44.9%) and H_2/CO ratio of 0.88 achieved at optimum conditions of reaction temperature 700 °C and feed ratio of 3.0.	[189]
CCD	i. CO_2:CH_4 ratio ii. GHSV iii. O_2 feed concentration iv. Reaction temperature	i. CH_4 conversions ii. H_2 yield	$Ni–Co/MgO–ZrO_2$	CH_4 conversions of 88% and H_2 yield of 86% achieved at optimum conditions of 749 °C, GHSV of 145,190 mL/g h, CO_2:CH_4 ratio of 3 and O_2 content of 7.	[190]
2^3 FD	i. Fe loading ii. Ni loading iii. Reaction temperature	H_2 yield	$Ni–Fe/MgAl_2O_4$	Reduction of 61% in the amount of nickel without loss in yield of H_2.	[191]
CCD	i. CH_4:CO feed ratio ii. GHSV iii. Reaction temperature	CH_4 conversion	Ni–La@KCC-1	CH_4 conversions of 97% achieved at optimum conditions of 820 °C, GHSV of 35.5 L/g h and CO_2:CH_4 ratio of 2.5.	[17]
BBD	i. CH_4 partial pressure ii. CO_2 partial pressure iii. Reaction Temperature	i. CO yield ii. H_2 yield	Co/Sm_2O_3	Optimum CH_4 and CO_2 partial pressures of 47.9 and 48.9 kPa at 735 °C resulting in syngas yield of 79.4 and 79.0% for H_2 and CO, respectively.	[192]
CCD	i. Ni loading ii. La loading iii. Calcination temperature	CH_4 conversion	$La–Ba–Ni/CuyO_3$	Maximum methane conversion was achieved via calcine temperature of 700 °C.	[193]

Table 3 – (continued)

Exp. design	Input variables	Response	Catalysts	Optimal process performance	Ref.
CCD	i. Discharge power ii. Total flow rate iii. CO_2:CH_4 molar ratio iv. Ni loading	i. CO2 conversion ii. CH_4 conversion iii. CO yield iv. H_2 yield	Ni/γ-Al_2O_3	Gas flow rate of 56.1 mL/min, a discharge power of 60.0 W, a CO_2:CH_4 molar ratio of 1.0 and a Ni loading of 9.5 wt%.	[194]

CCD: Central Composite Design; BBD: Box-Behnken Design; FD: Factorial Design; GHSV: Gas Hourly Space Velocity.

Table 4 – Reported pilot scale plants for DRM.

Plant	Year	Remarks	References
SPARG	1990	Production of syngas with H_2/CO ratio of unity via combination of steam, CO_2 and CH_4.	[199]
CALCOR	2001	Production of CO rich syngas.	[200]
Carbon Sciences Inc.	2010	Production of syngas using a bench top reactor.	[201]
Linde Group	2015	Production of syngas using Ni-based and Co-based catalysts.	[202]

a support material and subsequent stabilization of the active species within the pores is an effective strategy to ensure improved catalytic activity and stability against sintering. Ma et al. [207] have recently exemplified such strategy on Ni/Al_2O_3 using an evaporation-induced self-assembly method (EISA).

Obviously, diverse approaches have been reported which target effective stabilization of the Ni active phase against rapid deactivation. The key factors that contribute to fast decline in catalytic activity of DRM catalysts are majorly sintering and coke deposition, and they remain the great challenges to commercialization of a lot of catalysts. The incorporation of CeO_2 into the active phase of Ni/SiO_2 was recently found to promote the concentration of reactive oxygen species available for potential coke gasification in addition to weakening the metal-support interaction, leading to significant increase in the overall catalytic performance of the catalyst [208]. Depending on the nature of support, synergistic interplay due to creation of metal-support interface could provide a novel handle to tune DRM reactivity and stability of catalysts, as exemplified by Li et al. [209]. The authors confirmed that the formation of Ni–La_2O_3 interfacial synergy in a mesoporous Ni/La_2O_3 catalyst significantly promoted the evolution of active bidentate carbonates on the surface (Fig. 16a), as evident from combined *in situ* DRIFTS and DFT simulation. The bidentate carbons actively react with coke intermediates that are derived from methane activation. Such induced carbon deposition inhibition resulted to highly stable performance of the catalyst, as shown on Fig. 16b. Interestingly, NiFe bimetallic system supported on various materials is among the most promising DRM catalyst and a lot of efforts have been devoted towards improving its performance [210–212]. Jin et al. [213] found that controlled incorporation of Cu species can effectively enhance the Ni–Fe interaction (suppressing Fe segregation) in order to ensure adequate availability of labile oxygen to the Ni sites for coke removal over $Ni_3Fe_1Cu_1$-$Mg_xAl_yO_z$ catalyst. On another perspective, reaction conditions can equally be critical in regulating the structure-reactivity function of DRM catalysts via modulating the dynamic composition of the active phase, especially in perovskite-based catalytic systems. Shah et al. [214] revealed via HAADF-STEM and TPSR experiments found that the active phase of exsolved NiFeCo catalyst derived from La(Fe,Ni,Co)O_3 perovskite precursors was initially Fe-rich but became Ni- and Co-rich in the reactive atmosphere after 24 h time on stream. Most recently, Coster et al. [215] decipher a similar observation on Ni–Fe/$MgAl_2O_4$ catalyst via systematic *in situ* transmission QXAS measurements. The authors revealed that at CH_4/CO_2 < 1, FeO_x species were evidently generated on the active surface due to induced extraction of Fe from the Ni–Fe alloy, with some of the Fe potentially reincorporated into the support lattice, as depicted on Fig. 16c. At $CH_4/CO_2 = 1$, the CO_2-induced Fe segregation was significantly suppressed. This insightful interplay between the gas phase environment and dynamics in the composition of the active phase explains the reason for the stable DRM catalytic performance of a previously studied 8Ni_5Fe/$MgAl_2O_4$ under similar condition [216]. At the $CH_4/CO_2 = 1$ (a more reducing environment), large availability of CH_4 dissociation products countered oxidation of the Fe species by CO_2, thereby enabling improved stability of the Ni–Fe alloy phase that is beneficial in DRM.

Summary and perspectives

Remarkable research efforts have been made in modification of zeolite and clay based catalysts for DRM which indicate immense potentials for these materials. The swift deactivation of conventional zeolite catalysts in DRM is because of their high surface acidity which often lead to side reactions with inferior stability. Moreover, their shape and size selective attributes inhibits the diffusion of active metal crystallites into support channels, cracks and interstices, leading to

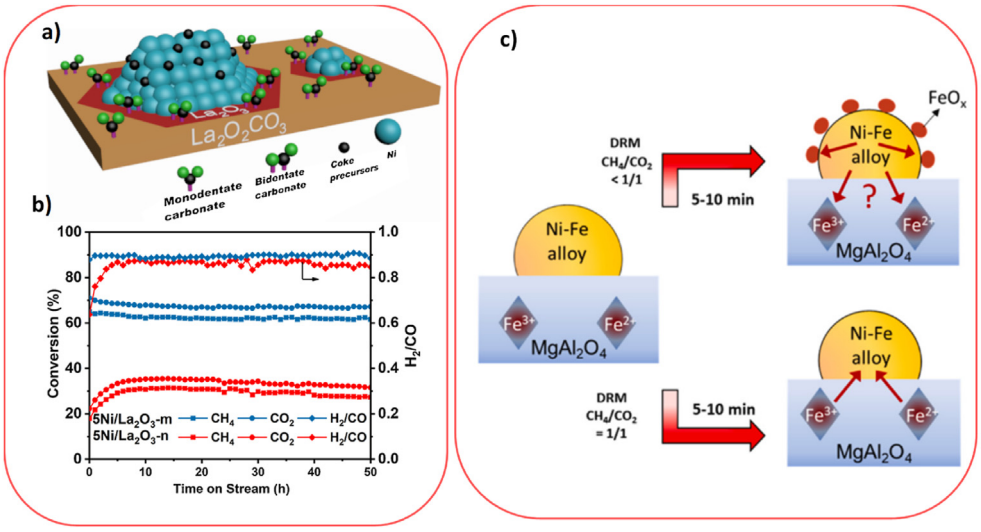

Fig. 16 – (a) A schematic model depicting the formation of bidentate carbon (BC) due to Ni–La_2O_3 interfacial synergy in a mesoporous Ni/La_2O_3 catalyst derived from templating SBA-15. The BC actively reacts with generate d coke precursor from methane activation. (b) Stable catalytic performance of the Ni/La_2O_3 catalyst during DRM. (c) Depiction of the dynamic changes in the composition of reduced 8$Ni_5Fe/MgAl_2O_4$ during DRM (750 °C, 1 atm, 30 min) with (B) CH_4/CO_2 < 1/1 and (C) CH_4/CO_2 = 1/1. The proposed model was developed from the useful insight obtained during *in situ* QXAS experiment. Reproduced from Ref. Li et al. [209] with permission from Elsevier.

accumulation of metal species on pore entrances. Restructuring of zeolite supports is a vital approach to introduce mesoporosity within the active phases which is prerequisite for robust DRM catalysts. Microemulsion, nitridation and one-pot are effective synthesis methods which could invoke high dispersion and stabilization of metal particles thereby boosting reactants accessibility to active sites. Conversely, spherically structured birdcage and fibrous zeolite supports are best explored with comparatively high activity, near unity H_2/CO ratio and remarkable stability under the harsh DRM conditions. Doping zeolite supported catalysts with promoters such as Ca, Ce, Mg, Gd, Ta, Ga, Co, Zr and La induced better Ni-support interaction and coking resistance. It was established that there is a correlation between coking resistance and the nature of acid-basic sites. Homogeneous distribution of acid-basic sites of zeolite catalysts lessens the tendency of carbon deposition due to comparable (CH_4 and CO_2) activation energy.

Several efforts on modification of clay materials are being explored. Selection of appropriate preparation method, treatment duration and calcination temperature played crucial role in dictating the performance of clay based catalysts in DRM. The use of organometallic functionalization synthesis route for deposition of the metal precursor on clay support is a vital approach in achieving high reaction rates for both reactants (CO_2 and CH_4) with superior stability. Calcination temperature is another crucial parameter in fine-tuning the final morphology of clay supported catalysts. Calcination at high temperature (~800 °C) produced superior stability with no noticeable coke formation in contrast to those calcined at low temperature (~500 °C). Also, pre-treatment condition plays a vital role on metal active sites formation, thus affecting catalytic performance. The catalysts reduced at low temperature produce better catalytic performance in contrast to the ones reduced at elevated temperature. Bimetallic design exemplified with Ni along with either Cu, Co, Ce, Mn and Fe phases over clay supports produced superior DRM activity and stability as a result of high reducibility and metal dispersion. In summary, the prerequisite for robust DRM catalyst system includes fine metal dispersion, good oxygen mobility, good metal support interaction, high surface area and basicity.

To better understand the correlations of process parameters with catalytic performance during DRM, an exhaustive analysis was conducted on reported studies with emphasis on optimization of process parameters using response surface methodology. Different feed ratio affects the product spectrum, where high CH_4 concentration in the feed induces production of syngas with higher H_2 content than CO and is accompanied by more carbon formation. Higher amount of CO_2 in the feed on the other hand drives the reaction in the direction of products with near unity H_2:CO ratio, and positively impact the catalyst life span.

It is undoubtable that engineering structured zeolite and clay based catalysts is attractive from both economical and industrial point of view. Among the possible DRM research focus include:

1. To explore new structured zeolite and clay supports with new morphologies by fine tuning the composition of the starting materials.
2. To explore more approaches in development of zeolite and clay supported catalysts with appropriate metallic formulations such as bi-metallic alloy formation with Ni and fourth period transition metals.
3. To examine deeply the interplay between structure-catalysis of zeolite and clay based catalysts in DRM reaction.
4. To experiment in practice the impact of co-feeding small traces of steam/oxygen with the DRM reactants since it

could thermodynamically affect product selectivity and carbon deposition.
5. To use computational modeling and advanced in-situ spectroscopy tools to further unravel the coking mechanism of DRM.

Concluding remarks

To circumvent catalyst deactivation associated with CO_2 reforming of methane, structured materials have been developed to support the active metal species. This review focused on zeolites and clays for such purposes, aiming to develop robust catalyst systems with high activity, stability and selectivity suitable for the industrialization of DRM process. These materials deserved attention due to their abundance, peculiar structures, high affinity for CO_2, environmentally friendly nature as well as tunable properties to improve selectivity of target products. Advances and perspectives in engineering mesostructured zeolite and clay supports with inclination to fine dispersion and immobilization of metal particles have greatly inspired hope towards development of cheap and efficient DRM catalysts. Using appropriate synthesis technique, composition of the starting materials, treatment duration, calcination protocol and promoters could pave way for development of a catalyst system with anti-coking and anti-sintering attributes which is prerequisite for robust DRM catalysts.

Declaration of competing interest

The authors declare that they have no known competing financial interests or personal relationships that could have appeared to influence the work reported in this paper.

Acknowledgements

The authors gratefully appreciate the support from University of Ilorin, Nigeria. We also like to acknowledge the funding from Universiti Teknologi Malaysia Transdisciplinary Grant (No. 06G52 and 06G53).

Nomenclature

ANOVA	Analysis of variance
BAS	Bronsted Acid Sites
MO	Metal oxides
MMO	Mixed metal oxides
CO_2-TPD	Carbon dioxide Temperature Programmed Desorption
CTAB	Cetyltrimethylammonium Bromide
CCUS	Carbon Capture, Utilization and Storage
CCS	Carbon Capture and Sequestration
CCU	Carbon Capture and Utilization
DFT	Density functional theory
DRM	Dy reforming of methane
EISA	Evaporation-induced self-assembly
FZSM-5	Fibrous ZSM-5
DTA	Differential Thermal Analysis
GHG	Greenhouse gases
GHSV	Gas Hourly Space Velocity
HAADF-STEM	High angle annular detector dark field scanning transmission microscopy
H_2-TPR	Hydrogen Temperature Programmed Reduction
KCC-1	KAUST Catalysis Centre 1
LAS	Lewis Acid Sites
MFI	Mordenite Framework Inverted
NH_3-TPD	Ammonia Temperature Programmed Desorption
RSM	Response Surface Methodology
RWGS	Reverse Water Gas Shift Reaction
SEM	Scanning Electron Microscopy
SPARG	Sulphur passivated reforming
SOMC	Surface Organometallic Chemistry
TEOS	Tetraethyl Orthosilicate
TGA	Thermogravimetric Analysis
TEM	Transmission Electron Microscopy
TPSR	Temperature Programmed Surface Reaction Spectroscopy
TOS	Time on stream
TPR	Temperature Programmed Reduction
XPS	X-ray photo electron spectroscopy
XRD	X-ray diffraction
ZSM-5	Zeolite Socony Mobil-5

REFERENCES

[1] Mohanty US, Ali M, Azhar MR, Al-Yaseri A, Keshavarz A, Iglauer S. Current advances in syngas (CO + H_2) production through bi-reforming of methane using various catalysts: a review. Int J Hydrogen Energy 2021;46:32809–45. https://doi.org/10.1016/j.ijhydene.2021.07.097.
[2] Siang TJ, Jalil AA, Abdulrahman A, Hambali HU. Enhanced carbon resistance and regenerability in methane partial oxidation to syngas using oxygen vacancy-rich fibrous Pd, Ru and Rh/KCC-1 catalysts. Environ Chem Lett 2021;19:2733–42. https://doi.org/10.1007/s10311-021-01192-0.
[3] Hussain I, Jalil AA, Hassan NS, Hambali HU, Jusoh NWC. Fabrication and characterization of highly active fibrous silica-mordenite (FS@SiO_2-MOR) cockscomb shaped catalyst for enhanced CO_2 methanation. Chem Eng Sci 2020;228:115978. https://doi.org/10.1016/j.ces.2020.115978.
[4] Al-Fatesh AS, Kumar R, Kasim SO, Ibrahim AA, Fakeeha AH, Abasaeed AE, et al. The effect of modifier identity on the performance of Ni-based catalyst supported on γ-Al_2O_3 in dry reforming of methane. Catal Today 2020;348:236–42. https://doi.org/10.1016/j.cattod.2019.09.003.
[5] Siang TJ, Jalil AA, Fatah NAA, Chung ME. Tailoring Rh content on dendritic fibrous silica alumina catalyst for enhanced CO_2 capture in catalytic CO_2 methanation. J Environ Chem Eng 2021;9:104616. https://doi.org/10.1016/j.jece.2020.104616.
[6] Siang TJ, Jalil AA, Hambali HU, Abdulrasheedand AA, Azami MS. Dendritic mesoporous Ni/KCC-1 for partial oxidation of methane to syngas. IOP Conf Ser Mater Sci Eng 2020;808. https://doi.org/10.1088/1757-899X/808/1/012006.
[7] Taherian Z, Gharahshiran VS, Fazlikhani F, Yousefpour M. Catalytic performance of Samarium-modified Ni catalysts

over Al_2O_3–CaO support for dry reforming of methane. Int J Hydrogen Energy 2021;46:7254–62. https://doi.org/10.1016/j.ijhydene.2020.11.196.
[8] Wysocka I, Mielewczyk-Gryń A, Łapiński M, Cieślik B, Rogala A. Effect of small quantities of potassium promoter and steam on the catalytic properties of nickel catalysts in dry/combined methane reforming. Int J Hydrogen Energy 2021;46:3847–64. https://doi.org/10.1016/j.ijhydene.2020.10.189.
[9] Abdulrasheed A, Jalil AA, Gambo Y, Ibrahim M, Hambali HU, Shahul Hamid MY. A review on catalyst development for dry reforming of methane to syngas: recent advances. Renew Sustain Energy Rev 2019;108:175–93. https://doi.org/10.1016/j.rser.2019.03.054.
[10] Wittich K, Krämer M, Bottke N, Schunk SA. Catalytic dry reforming of methane: insights from model systems. ChemCatChem 2020. https://doi.org/10.1002/cctc.201902142.
[11] Pakhare D, Shaw C, Haynes D, Shekhawat D, Spivey J. Effect of reaction temperature on activity of Pt- and Ru-substituted lanthanum zirconate pyrochlores ($La_2Zr_2O_7$) for dry (CO_2) reforming of methane (DRM). J CO_2 Util 2013;1:37–42. https://doi.org/10.1016/j.jcou.2013.04.001.
[12] Yusuf M, Farooqi AS, Al-Kahtani AA, Ubaidullah M, Alam MA, Keong LK, et al. Syngas production from greenhouse gases using Ni–W bimetallic catalyst via dry methane reforming: effect of W addition. Int J Hydrogen Energy 2021;46:27044–61. https://doi.org/10.1016/j.ijhydene.2021.05.186.
[13] Al-Fatesh AS, Fakeeha AH, Ibrahim AA, Abasaeed AE. Ni supported on La_2O_3+ZrO_2 for dry reforming of methane: the impact of surface adsorbed oxygen species. Int J Hydrogen Energy 2021;46:3780–8. https://doi.org/10.1016/j.ijhydene.2020.10.164.
[14] Aramouni NAK, Touma JG, Tarboush BA, Zeaiter J, Ahmad MN. Catalyst design for dry reforming of methane: analysis review. Renew Sustain Energy Rev 2018;82:2570–85. https://doi.org/10.1016/j.rser.2017.09.076.
[15] Abdulrasheed AA, Jalil AA, Hamid MYS, Siang TJ, Fatah NAA, Izan SM, et al. Dry reforming of methane to hydrogen-rich syngas over robust fibrous KCC-1 stabilized nickel catalyst with high activity and coke resistance. Int J Hydrogen Energy 2020;45:18549–61. https://doi.org/10.1016/j.ijhydene.2019.04.126.
[16] Hambali HU, Jalil AA, Abdulrasheed AA, Siang TJ, Nyakuma BB, Nabgan W, et al. Effect of Ni-Ta ratio on the catalytic selectivity of fibrous Ni-Ta/ZSM-5 for dry reforming of methane. Chem Eng Sci 2020;227:115952. https://doi.org/10.1016/j.ces.2020.115952.
[17] Abdulrasheed AA, Jalil AA, Hamid MYS, Siang TJ, Abdullah TAT. Dry reforming of CH_4 over stabilized Ni-La@KCC-1 catalyst: effects of la promoter and optimization studies using RSM. J CO_2 Util 2020;37:230–9. https://doi.org/10.1016/j.jcou.2019.12.018.
[18] Horlyck J, Lawrey C, Lovell EC, Amal R, Scott J. Elucidating the impact of Ni and Co loading on the selectivity of bimetallic NiCo catalysts for dry reforming of methane. Chem Eng J 2018;352:572–80. https://doi.org/10.1016/j.cej.2018.07.009.
[19] Chong CC, Cheng YW, Setiabudi HD, Ainirazali N, Vo DVN, Abdullah B. Dry reforming of methane over Ni/dendritic fibrous SBA-15 (Ni/DFSBA-15): optimization, mechanism, and regeneration studies. Int J Hydrogen Energy 2020;45:8507–25. https://doi.org/10.1016/j.ijhydene.2020.01.056.
[20] Farooqi AS, Yusuf M, Mohd Zabidi NA, Saidur R, Sanaullah K, Farooqi AS, et al. A comprehensive review on improving the production of rich-hydrogen via combined steam and CO_2 reforming of methane over Ni-based catalysts. Int J Hydrogen Energy 2021;46:31024–40. https://doi.org/10.1016/j.ijhydene.2021.01.049.
[21] Usman M, Daud WMAW, Abbas HF. Dry reforming of methane : influence of process parameters — a review. Renew Sustain Energy Rev 2015;45:710–44. https://doi.org/10.1016/j.rser.2015.02.026.
[22] Schwab E, Milanov A, Schunk SA, Behrens A, Schödel N. Dry reforming and reverse water gas shift: alternatives for syngas production? Chem Ing Tech 2015;87:347–53. https://doi.org/10.1002/cite.201400111.
[23] Er-Rbib H, Bouallou C, Werkoff F. Production of synthetic gasoline and diesel fuel from dry reforming of methane. Energy Proc 2012;29:156–65. https://doi.org/10.1016/j.egypro.2012.09.020.
[24] Sittichompoo S, Nozari H, Herreros JM, Serhan N, da Silva JAM, York APE, et al. Exhaust energy recovery via catalytic ammonia decomposition to hydrogen for low carbon clean vehicles. Fuel 2021;285. https://doi.org/10.1016/j.fuel.2020.119111.
[25] Kosinov N, Liu C, Hensen EJM, Pidko EA. Engineering of transition metal catalysts confined in zeolites. Chem Mater 2018;30:3177–98. https://doi.org/10.1021/acs.chemmater.8b01311.
[26] Aziz MAH, Jalil AA, Siang TJ, Hussain I, Rahman AFA, Hamdan H. Abundant Lewis acidic sites of peculiar fibrous silica zeolite X enhanced toluene conversion in side chain toluene methylation. Fuel 2021;305:121432. https://doi.org/10.1016/j.fuel.2021.121432.
[27] Rahman AFA, Jalil AA, Hitam CNC, Hassan NS, Mohamed M, Hambali HU. Influence of dendrimeric silica BEA zeolite towards acidity and mesoporosity for enhanced benzene methylation. Mater Today Proc 2019;42:211–6. https://doi.org/10.1016/j.matpr.2020.11.589.
[28] Fatah NAA, Jalil AA, Firmansyah ML, Triwahyono S, Setiabudi HD, Vo DVN. Enhanced hydrogen-assisted cracking of 1,3,5-triisopropylbenzene over fibrous silica ZSM-5: influence of co-surfactant during synthesis. Int J Hydrogen Energy 2021;46:24676–86. https://doi.org/10.1016/j.ijhydene.2019.12.215.
[29] Hambali HU, Jalil AA, Triwahyono S, Jamian SF, Fatah NAA, Abdulrasheed AA, et al. Unique structure of fibrous ZSM-5 catalyst expedited prolonged hydrogen atom restoration for selective production of propylene from methanol. Int J Hydrogen Energy 2021;46:24652–65. https://doi.org/10.1016/j.ijhydene.2019.11.236.
[30] Kweon S, An H, Shin C, Park MB, Min H. Nitrided Ni/N-zeolites as efficient catalysts for the dry reforming of methan. J CO_2 Util 2021;46:101478. https://doi.org/10.1016/j.jcou.2021.101478.
[31] Kobayashi T, Furuya T, Fujitsuka H, Tago T. Synthesis of Birdcage-type zeolite encapsulating ultrafine Pt nanoparticles and its application in dry reforming of methane. Chem Eng J 2019;377:120203. https://doi.org/10.1016/j.cej.2018.10.140.
[32] Masudi A, Jusoh NWC, Muraza O. Opportunities for less-explored zeolitic materials in the syngas-to-olefins pathway over nanoarchitectured catalysts: a mini review. Catal Sci Technol 2020;10:1582–96. https://doi.org/10.1039/C9CY01875A.
[33] Saka C, Eygi MS, Balbay A. Cobalt loaded organic acid modified kaolin clay for the enhanced catalytic activity of hydrogen release via hydrolysis of sodium borohydride. Int J Hydrogen Energy 2021;46:3876–86. https://doi.org/10.1016/j.ijhydene.2020.10.201.
[34] Ayodele OB, Abdullah AZ. Exploring kaolinite as dry methane reforming catalyst support: influences of chemical activation, organic ligand functionalization and calcination

temperature. Appl Catal Gen 2019;576:20–31. https://doi.org/10.1016/j.apcata.2019.02.034.
[35] Lazaratou CV, Vayenas DV, Papoulis D. The role of clays, clay minerals and clay-based materials for nitrate removal from water systems: a review. Appl Clay Sci 2020;185:105377. https://doi.org/10.1016/j.clay.2019.105377.
[36] Hossain MA, Ayodele BV, Cheng CK, Khan MR. Optimization of renewable hydrogen-rich syngas production from catalytic reforming of greenhouse gases (CH_4 and CO_2) over calcium iron oxide supported nickel catalyst. J Energy Inst 2019;92:177–94. https://doi.org/10.1016/j.joei.2017.10.010.
[37] Abdullah B, Azeanni N, Ghani A, Vo DN. Recent advances in dry reforming of methane over Ni-based catalysts. J Clean Prod 2017;162:170–85. https://doi.org/10.1016/j.jclepro.2017.05.176.
[38] Wang B, Albarracín-Suazo S, Pagán-Torres Y, Nikolla E. Advances in methane conversion processes. Catal Today 2017;285:147–58. https://doi.org/10.1016/j.cattod.2017.01.023.
[39] Chong CC, Cheng YW, Bahari MB, Teh LP, Abidin SZ, Setiabudi HD. Development of nanosilica-based catalyst for syngas production via CO_2 reforming of CH_4: a review. Int J Hydrogen Energy 2020. https://doi.org/10.1016/j.ijhydene.2020.01.086.
[40] Das S, Pérez-Ramírez J, Gong J, Dewangan N, Hidajat K, Gates BC, et al. Core-shell structured catalysts for thermocatalytic, photocatalytic, and electrocatalytic conversion of CO_2. Chem Soc Rev 2020;49:2937–3004. https://doi.org/10.1039/c9cs00713j.
[41] Bian Z, Wang Z, Jiang B, Hongmanorom P, Zhong W, Kawi S. A review on perovskite catalysts for reforming of methane to hydrogen production. Renew Sustain Energy Rev 2020;134:110291. https://doi.org/10.1016/j.rser.2020.110291.
[42] Siang TJ, Jalil AA, Hambali HU, Hussain I, Saifulddin M. Catalytic partial oxidation of methane to syngas over perovskite catalysts, vol. 90; 2019, 01006. https://doi.org/10.1051/e3sconf/20199001006.
[43] Liu H, Hadjltaief HB, Benzina M, Gálvez ME, Da Costa P. Natural clay based nickel catalysts for dry reforming of methane: on the effect of support promotion (La, Al, Mn). Int J Hydrogen Energy 2019;4:246–55. https://doi.org/10.1016/j.ijhydene.2018.03.004.
[44] Nyakuma BB, Wong SL, Oladokun O, Bello AA, Hambali HU, Abdullah TAT, et al. Review of the fuel properties, characterisation techniques, and pre-treatment technologies for oil palm empty fruit bunches. Biomass Convers Biorefinery 2020. https://doi.org/10.1007/s13399-020-01133-x.
[45] Ghanbari T, Abnisa F, Wan Daud WMA. A review on production of metal organic frameworks (MOF) for CO_2 adsorption. Sci Total Environ 2020;707:135090. https://doi.org/10.1016/j.scitotenv.2019.135090.
[46] Rogelj J, Den Elzen M, Höhne N, Fransen T, Fekete H, Winkler H, et al. Paris Agreement climate proposals need a boost to keep warming well below 2 °c. Nature 2016;534:631–9. https://doi.org/10.1038/nature18307.
[47] Xu J, Xia P, Zhang Q, Guo F, Xia Y, Tian H. Coke resistance of Ni-based catalysts enhanced by cold plasma treatment for CH4–CO2 reforming: Review. Int J Hydrogen Energy 2021;46:23174–89. https://doi.org/10.1016/j.ijhydene.2021.03.245.
[48] Hambali HU, Jalil AA, Abdulrasheed AA, Siang TJ, Abdullah TAT, Ahmad A, et al. Fibrous spherical Ni-M/ZSM-5 (M: Mg, Ca, Ta, Ga) catalysts for methane dry reforming: the interplay between surface acidity-basicity and coking resistance. Int J Energy Res 2020:1–17. https://doi.org/10.1002/er.5327.
[49] Bawah AR, Lucky RA, Hossain MM. Oxidative dehydrogenation of propane with CO_2 - a green process for propylene and hydrogen (syngas). Int J Hydrogen Energy 2021;46:3401–13. https://doi.org/10.1016/j.ijhydene.2020.10.168.
[50] Ma S, Chen G, Guo M, Zhao L, Han T, Zhu S. Path analysis on CO_2 resource utilization based on carbon capture using ammonia method in coal-fired power Plants. Renew Sustain Energy Rev 2014;37:687–97. https://doi.org/10.1016/j.rser.2014.05.048.
[51] Alper E, Yuksel Orhan O. CO_2 utilization: developments in conversion processes. Petroleum 2017;3:109–26. https://doi.org/10.1016/j.petlm.2016.11.003.
[52] Norhasyima RS, Mahlia TMI. Advances in CO_2 utilization technology: a patent landscape review. J CO_2 Util 2018;26:323–35. https://doi.org/10.1016/j.jcou.2018.05.022.
[53] Tarkowski R, Uliasz-Misiak B, Tarkowski P. Storage of hydrogen, natural gas, and carbon dioxide – geological and legal conditions. Int J Hydrogen Energy 2021;46:20010–22. https://doi.org/10.1016/j.ijhydene.2021.03.131.
[54] Ali Khan MH, Daiyan R, Neal P, Haque N, MacGill I, Amal R. A framework for assessing economics of blue hydrogen production from steam methane reforming using carbon capture storage & utilisation. Int J Hydrogen Energy 2021;46:22685–706. https://doi.org/10.1016/j.ijhydene.2021.04.104.
[55] Bui M, Adjiman CS, Bardow A, Anthony EJ, Boston A, Brown S, et al. Carbon capture and storage (CCS): the way forward. Energy Environ Sci 2018;11:1062–176. https://doi.org/10.1039/c7ee02342a.
[56] Cormos AM, Dinca C, Petrescu L, Andreea Chisalita D, Szima S, Cormos CC. Carbon capture and utilisation technologies applied to energy conversion systems and other energy-intensive industrial applications. Fuel 2018;211:883–90. https://doi.org/10.1016/j.fuel.2017.09.104.
[57] Egeland-Eriksen T, Hajizadeh A, Sartori S. Hydrogen-based systems for integration of renewable energy in power systems: achievements and perspectives. Int J Hydrogen Energy 2021;46:31963–83. https://doi.org/10.1016/j.ijhydene.2021.06.218.
[58] Fernández-Amador O, Francois JF, Oberdabernig DA, Tomberger P. The methane footprint of nations: stylized facts from a global panel dataset. Ecol Econ 2020;170:106528. https://doi.org/10.1016/j.ecolecon.2019.106528.
[59] Horn R, Schlögl R. Methane activation by heterogeneous catalysis. Catal Lett 2015;145:23–39. https://doi.org/10.1007/s10562-014-1417-z.
[60] Suyetin M, Peskov MV, Schwingenschlögl U. Methane sorption in a family of qzd-MOFs: a multiscale computational study. Chem Eng J 2020;384:123296. https://doi.org/10.1016/j.cej.2019.123296.
[61] Das S, Sengupta M, Patel J, Bordoloi A. A study of the synergy between support surface properties and catalyst deactivation for CO_2 reforming over supported Ni nanoparticles. Appl Catal Gen 2017;545:113–26. https://doi.org/10.1016/j.apcata.2017.07.044.
[62] Hambali HU, Jalil AA, Abdulrasheed AA, Siang TJ, Owgi AHK, Aziz FFA. CO_2 reforming of methane over Ta-promoted Ni/ZSM-5 fibre-like catalyst: insights on deactivation behavior and optimization using response surface methodology (RSM). Chem Eng Sci 2021;231:116320. https://doi.org/10.1016/j.ces.2020.116320.
[63] Karakaya C, Kee RJ. Progress in the direct catalytic conversion of methane to fuels and chemicals. Prog Energy Combust Sci 2016;55:60–97. https://doi.org/10.1016/j.pecs.2016.04.003.

[64] Wang M, Zhang Q, Zhang T, Wang Y, Wang J, Long K, et al. Facile one-pot synthesis of highly dispersed Ni nanoparticles embedded in HMS for dry reforming of methane. Chem Eng J 2017;313:1370–81. https://doi.org/10.1016/j.cej.2016.11.055.
[65] Gambo Y, Adamu S, Abdulrasheed AA, Lucky RA, Ba-Shammakh MS, Hossain MM. Catalyst design and tuning for oxidative dehydrogenation of propane – a review. Appl Catal Gen 2021;609:117914. https://doi.org/10.1016/j.apcata.2020.117914.
[66] Wang Y, Yao L, Wang S, Mao D, Hu C. Low-temperature catalytic CO_2 dry reforming of methane on Ni-based catalysts: a review. Fuel Process Technol 2018;169:199–206. https://doi.org/10.1016/j.fuproc.2017.10.007.
[67] Li Z, Das S, Hongmanorom P, Dewangan N, Wai MH, Kawi S. Silica-based micro- and mesoporous catalysts for dry reforming of methane. Catal Sci Technol 2018;8:2763–78. https://doi.org/10.1039/c8cy00622a.
[68] Hambali HU, Jalil AA, Abdulrasheed AA, Siang TJ, Vo D-VN. Enhanced dry reforming of methane over mesostructured fibrous Ni/MFI zeolite: influence of preparation methods. J Energy Inst 2020. https://doi.org/10.1016/j.joei.2020.01.016.
[69] Bawah AR, Malaibari ZO, Muraza O. Syngas production from CO_2 reforming of methane over Ni supported on hierarchical silicalite-1 fabricated by microwave-assisted hydrothermal synthesis. Int J Hydrogen Energy 2018;43:13177–89. https://doi.org/10.1016/j.ijhydene.2018.05.073.
[70] Abdulrasheed AA, Jalil AA, Siang TJ, Hambali HU. T Thermodynamic sensitivity analysis of CO_2 reforming of methane based on equilibrium predictions. IOP Conf Ser Mater Sci Eng 2020. https://doi.org/10.1088/1757-899X/808/1/012001.
[71] Hambali HU, Jalil AA, Abdulrasheed AA, Siang TJ, Fatah NAA, Rahman AFA, et al. Effect of transition metals (Mo, Mn and Co) on mesoporous ZSM-5 catalyst activity in carbon dioxide reforming of methane. IOP Conf Ser Mater Sci Eng 2020. https://doi.org/10.1088/1757-899X/808/1/012005.
[72] Giehr A, Maier L, Schunk SA, Deutschmann O. Thermodynamic considerations on the oxidation state of Co/γ-Al_2O_3 and Ni/γ-Al_2O_3 catalysts under dry and steam reforming conditions. ChemCatChem 2018;10:751–7. https://doi.org/10.1002/cctc.201701376.
[73] Schulz LA, Kahle LCS, Delgado KH, Schunk SA, Jentys A, Deutschmann O, et al. On the coke deposition in dry reforming of methane at elevated pressures. Appl Catal Gen 2015;504:599–607. https://doi.org/10.1016/j.apcata.2015.03.002.
[74] Takenaka S, Kato E, Tomikubo Y, Otsuka K. Structural change of Ni species during the methane decomposition and the subsequent gasification of deposited carbon with CO_2 over supported Ni catalysts. J Catal 2003;219:176–85. https://doi.org/10.1016/S0021-9517(03)00152-0.
[75] Wang Z, Cao XM, Zhu J, Hu P. Activity and coke formation of nickel and nickel carbide in dry reforming: a deactivation scheme from density functional theory. J Catal 2014;311:469–80. https://doi.org/10.1016/j.jcat.2013.12.015.
[76] Chong CC, Cheng YW, Bukhari SN, Setiabudi HD, Jalil AA. Methane dry reforming over Ni/fibrous SBA-15 catalysts: effects of support morphology (rod-liked F-SBA-15 and dendritic DFSBA-15). Catal Today 2021;375:245–57. https://doi.org/10.1016/j.cattod.2020.06.073.
[77] Muraza O, Galadima A. A review on coke management during dry reforming of methane. Int J Energy Res 2015. https://doi.org/10.1002/er.3295.
[78] Rahman AFA, Jalil AA, Jusoh NWC, Mohamed M, Fatah NAA, Hambali HU. Shape selective alkylation of benzene with methanol over different zeolite catalysts. IOP Conf Ser Mater Sci Eng 2020. https://doi.org/10.1088/1757-899X/808/1/012003.
[79] Hambali HU, Jalil AA, Siang TJ, Abdulrasheed AA, Fatah NAA, Hussain I, et al. Effect of ZSM-5 acidity in enhancement of methanol-to-olefins. Processes 2019;4:9–13.
[80] Aziz MAH, Jalil AA, Hambali HU, Rahman AFA. Hydrogenation of methanol to olefins over highly stable ruthenium oxide protonated fibrous ZSM5 catalyst. IOP Conf Ser Mater Sci Eng 2020. https://doi.org/10.1088/1757-899X/736/4/042031.
[81] Estephane J, Aouad S, Hany S, El Khoury B, Gennequin C, El Zakhem H, et al. CO_2 reforming of methane over Ni-Co/ZSM5 catalysts. Aging and carbon deposition study. Int J Hydrogen Energy 2015;40:9201–8. https://doi.org/10.1016/j.ijhydene.2015.05.147.
[82] Sarkar B, Tiwari R, Singha RK, Suman S, Ghosh S, Acharyya SS, et al. Reforming of methane with CO_2 over Ni nanoparticle supported on mesoporous ZSM-5. Catal Today 2012;198:209–14. https://doi.org/10.1016/j.cattod.2012.04.029.
[83] Abdollahifar M, Haghighi M, Sharifi M. Dry reforming of methane over nanostructured Co/Y catalyst for hydrogen production: effect of ultrasound irradiation and Co-loading on catalyst properties and performance. Energy Convers Manag 2015;103:1101–12. https://doi.org/10.1016/j.enconman.2015.04.053.
[84] Jalil AA, Gambo Y, Abdulrasheed AA, Asli UA. Platinum - promoted fibrous silica Y zeolite with enhanced mass transfer as a highly selective catalyst for n - dodecane hydroisomerization. Int J Energy Res 2019:1–16. https://doi.org/10.1002/er.4545.
[85] Galadima A, Muraza O. Zeolite catalyst design for the conversion of glucose to furans and other renewable fuels. Fuel 2019;258:115851. https://doi.org/10.1016/j.fuel.2019.115851.
[86] Kawi S, Kathiraser Y, Ni J, Oemar U, Li Z, Saw ET. Progress in synthesis of highly active and stable nickel-based catalysts for carbon dioxide reforming of methane. ChemSusChem 2015;8:3556–75. https://doi.org/10.1002/cssc.201500390.
[87] Ahmed AH. Zeolite-encapsulated transition metal chelates: synthesis and characterization. Rev Inorg Chem 2014;34:153–75. https://doi.org/10.1515/revic-2013-0013.
[88] Degnan TF, Chitnis GK, Schipper PH. History of ZSM-5 fluid catalytic cracking additive development at Mobil. Microporous Mesoporous Mater 2000;35–36:245–52. https://doi.org/10.1016/S1387-1811(99)00225-5.
[89] Wei Q, Yang G, Gao X, Yamane N, Zhang P, Liu G, et al. Ni/Silicalite-1 coating being coated on SiC foam: a tailor-made monolith catalyst for syngas production using a combined methane reforming process. Chem Eng J 2017;327:465–73. https://doi.org/10.1016/j.cej.2017.06.109.
[90] Hao Z, Zhu HY, Lu GQ. Zr-Laponite pillared clay-based nickel catalysts for methane reforming with carbon dioxide. Appl Catal Gen 2003;242:275–86. https://doi.org/10.1016/S0926-860X(02)00519-7.
[91] Li B, Lin X, Luo Y, Yuan X, Wang X. Design of active and stable bimodal nickel catalysts for methane reforming with CO2. Fuel Process Technol 2018;176:153–66. https://doi.org/10.1016/j.fuproc.2018.03.032.
[92] Amin MH, Sudarsanam P, Field MR, Patel J, Bhargava SK. Effect of a swelling agent on the performance of Ni/porous silica catalyst for CH_4-CO_2 reforming. Langmuir 2017;33:10632–44. https://doi.org/10.1021/acs.langmuir.7b02753.
[93] Li B, Yuan X, Li B, Wang X. Impact of pore structure on hydroxyapatite supported nickel catalysts (Ni/HAP) for dry reforming of methane. Fuel Process Technol

2020;202:106359. https://doi.org/10.1016/j.fuproc.2020.106359.
[94] Aziz A, Jalil AA, Wongsakulphasatch S, Vo D-V N. Understanding the role of surface basic sites of catalyst in Co_2 activation of dry reforming of methane: a short review. Catal Sci Technol 2019:35–45. https://doi.org/10.1039/C9CY01519A.
[95] Budiman AW, Song SH, Chang TS, Shin CH, Choi MJ. Dry reforming of methane over cobalt catalysts: a literature review of catalyst development. Catal Surv Asia 2012;16:183–97. https://doi.org/10.1007/s10563-012-9143-2.
[96] Huang T, Huang W, Huang J, Ji P. Methane reforming reaction with carbon dioxide over SBA-15 supported Ni-Mo bimetallic catalysts. Fuel Process Technol 2011;92:1868–75. https://doi.org/10.1016/j.fuproc.2011.05.002.
[97] Alipour Z, Rezaei M, Meshkani F. Effect of Ni loadings on the activity and coke formation of MgO-modified Ni/Al_2O_3 nanocatalyst in dry reforming of methane. J Energy Chem 2014;23:633–8. https://doi.org/10.1016/S2095-4956(14)60194-7.
[98] Ennaert T, Van Aelst J, Dijkmans J, De Clercq R, Schutyser W, Dusselier M, Verboekend D, Sels BF. Potential and challenges of zeolite chemistry in the catalytic conversion of biomass. Chem Soc Rev 2016;45:584–611. https://doi.org/10.1039/C5CS00859J.
[99] Ni J, Chen L, Lin J, Kawi S. Carbon deposition on borated alumina supported nano-sized Ni catalysts for dry reforming of CH_4. Nano Energy 2012;1:674–86. https://doi.org/10.1016/j.nanoen.2012.07.011.
[100] Tang M, Xu L, Fan M. Effect of Ce on 5 wt% Ni/ZSM-5 catalysts in the CO_2 reforming of CH4 reaction. Int J Hydrogen Energy 2014;39:15482–96. https://doi.org/10.1016/j.ijhydene.2014.07.172.
[101] Jeong H, Kim KI, Kim D, Song IK. Effect of promoters in the methane reforming with carbon dioxide to synthesis gas over Ni/HY catalysts. J Mol Catal Chem 2006;246:43–8. https://doi.org/10.1016/j.molcata.2005.10.013.
[102] Al-Fatesh AS, Atia Hanan, Ibrahim AA, Fakeeha AH, Singh SK, Labhsetwar NK, et al. CO_2 reforming of CH4: effect of Gd as promoter for Ni supported over MCM-41 as catalyst. Renew Energy 2019;140:658–67. https://doi.org/10.1016/j.renene.2019.03.082.
[103] Liu D, Lau R, Borgna A, Yang Y. Carbon dioxide reforming of methane to synthesis gas over Ni-MCM-41 catalysts. Appl Catal Gen 2009;358:110–8. https://doi.org/10.1016/j.apcata.2008.12.044.
[104] Stroud T, Smith TJ, Le Saché E, Santos JL, Centeno MA, Arellano-Garcia H, et al. Chemical CO_2 recycling via dry and bi reforming of methane using $Ni-Sn/Al_2O_3$ and $Ni-Sn/CeO_2-Al_2O_3$ catalysts. Appl Catal B Environ 2018;224:125–35. https://doi.org/10.1016/j.apcatb.2017.10.047.
[105] Abou Rached J, Cesario MR, Estephane J, Tidahy HL, Gennequin C, Aouad S, et al. Effects of cerium and lanthanum on Ni-based catalysts for CO_2 reforming of toluene. J Environ Chem Eng 2018;6:4743–54. https://doi.org/10.1016/j.jece.2018.06.054.
[106] Zhang Q, Zhang T, Shi Y, Zhao B, Wang M, Liu Q, et al. A sintering and carbon-resistant Ni-SBA-15 catalyst prepared by solid-state grinding method for dry reforming of methane. J CO_2 Util 2017;17:10–9. https://doi.org/10.1016/j.jcou.2016.11.002.
[107] Davis ME. Ordered porous materials for emerging applications. Nature 2002;417:813–21. https://doi.org/10.1038/nature00785.
[108] Saraswat SK, Pant KK. Ni-Cu-Zn/MCM-22 catalysts for simultaneous production of hydrogen and multiwall carbon nanotubes via thermo-catalytic decomposition of methane. Int J Hydrogen Energy 2011;36:13352–60. https://doi.org/10.1016/j.ijhydene.2011.07.102.
[109] Frontera P, Macario A, Aloise A, Antonucci PL, Giordano G, Nagy JB. Effect of support surface on methane dry-reforming catalyst preparation. Catal Today 2013;218–219:18–29. https://doi.org/10.1016/j.cattod.2013.04.029.
[110] Singh S, Kumar R, Setiabudi HD, Nanda S, Vo DVN. Advanced synthesis strategies of mesoporous SBA-15 supported catalysts for catalytic reforming applications: a state-of-the-art review. Appl Catal Gen 2018;559:57–74. https://doi.org/10.1016/j.apcata.2018.04.015.
[111] Zhao W, Chen F-E. One-pot synthesis and its practical application in pharmaceutical industry. Curr Org Synth 2013;9:873–97. https://doi.org/10.2174/157017912803901619.
[112] Lovell E, Jiang Y, Scott J, Wang F, Suhardja Y, Chen M, et al. CO_2 reforming of methane over MCM-41-supported nickel catalysts: altering support acidity by one-pot synthesis at room temperature. Appl Catal Gen 2014;473:51–8. https://doi.org/10.1016/j.apcata.2013.12.020.
[113] Vafaeian Y, Haghighi M, Aghamohammadi S. Ultrasound assisted dispersion of different amount of Ni over ZSM-5 used as nanostructured catalyst for hydrogen production via CO_2 reforming of methane. Energy Convers Manag 2013;76:1093–103. https://doi.org/10.1016/j.enconman.2013.08.010.
[114] Frontera P, Aloise A, MacArio A, Antonucci PL, Crea F, Giordano G, et al. Bimetallic zeolite catalyst for CO_2 reforming of methane. Top Catal 2010;53:265–72. https://doi.org/10.1007/s11244-009-9409-8.
[115] Pakhare D, Spivey J. A review of dry (CO2) reforming of methane over noble metal catalysts. Chem Soc Rev 2014. https://doi.org/10.1039/c3cs60395d.
[116] Dai C, Zhang S, Zhang A, Song C, Shi C, Guo X. Hollow zeolite encapsulated Ni-Pt bimetals for sintering and coking resistant dry reforming of methane. J Math Chem 2015;3:16461. https://doi.org/10.1039/c5ta03565a.
[117] Miedziak PJ, Kondrat SA, Sajjad N, King GM, Douthwaite M, Shaw G, et al. Physical mixing of metal acetates: optimisation of catalyst parameters to produce highly active bimetallic catalysts. Catal Sci Technol 2013;3:2910–7. https://doi.org/10.1039/c3cy00263b.
[118] Miranda-Trevino JC, Coles CA. Kaolinite properties, structure and influence of metal retention on pH. Appl Clay Sci 2003;23:133–9. https://doi.org/10.1016/S0169-1317(03)00095-4.
[119] Lee SM, Tiwari D. Organo and inorgano-organo-modified clays in the remediation of aqueous solutions: an overview. Appl Clay Sci 2012;59–60:84–102. https://doi.org/10.1016/j.clay.2012.02.006.
[120] Dewangan N, Hui WM, Jayaprakash S, Bawah AR, Poerjoto AJ, Jie T, et al. Recent progress on layered double hydroxide (LDH) derived metal-based catalysts for CO_2 conversion to valuable chemicals. Catal Today 2020;356:490–513. https://doi.org/10.1016/j.cattod.2020.06.020.
[121] Sanusi OM, Benelfellah A, Aït Hocine N. Clays and carbon nanotubes as hybrid nanofillers in thermoplastic-based nanocomposites – a review. Appl Clay Sci 2020;185. https://doi.org/10.1016/j.clay.2019.105408.
[122] Melo CR, Riella HG, Kuhnen NC, Angioletto E, Melo AR, Bernardin AM, et al. Synthesis of 4A zeolites from kaolin for obtaining 5A zeolites through ionic exchange for adsorption of arsenic. Mater Sci Eng B Solid-State Mater Adv Technol 2012;177:345–9. https://doi.org/10.1016/j.mseb.2012.01.015.
[123] Ayodele OB, Sulaimon AA, Alaba PA, Tian ZY. Influence of metakaolinization temperature on the structure and activity of metakaolin supported Ni catalyst in dry methane

reforming. J Environ Chem Eng 2020;8:103239. https://doi.org/10.1016/j.jece.2019.103239.
[124] Zhou Z, Jin G, Liu H, Wu J, Mei J. Crystallization mechanism of zeolite A from coal kaolin using a two-step method. Appl Clay Sci 2014;97–98:110–4. https://doi.org/10.1016/j.clay.2014.05.015.
[125] Belver C, Bañares Muñoz MA, Vicente MA. Chemical activation of a kaolinite under acid and alkaline conditions. Chem Mater 2002;14:2033–43. https://doi.org/10.1021/cm0111736.
[126] Ayodele OB, Lim JK, Hameed BH. Degradation of phenol in photo-Fenton process by phosphoric acid modified kaolin supported ferric-oxalate catalyst: optimization and kinetic modeling. Chem Eng J 2012;197:181–92. https://doi.org/10.1016/j.cej.2012.04.053.
[127] Ayodele OB. Effect of phosphoric acid treatment on kaolinite supported ferrioxalate catalyst for the degradation of amoxicillin in batch photo-Fenton process. Appl Clay Sci 2013;72:74–83. https://doi.org/10.1016/j.clay.2013.01.004.
[128] Margossian T, Larmier K, Kim SM, Krumeich F, Fedorov A, Chen P, et al. Molecularly tailored nickel precursor and support yield a stable methane dry reforming catalyst with superior metal utilization. J Am Chem Soc 2017;139:6919–27. https://doi.org/10.1021/jacs.7b01625.
[129] Nicola BP, Schwanke AJ, Bernardo-Gusmão K. Porous clay nanoarchitectures as supports for heterogenized nickel complexes in catalytic reactions of ethylene oligomerization. Catal Today 2021. https://doi.org/10.1016/j.cattod.2021.08.028.
[130] Copéret C, Comas-Vives A, Conley MP, Estes DP, Fedorov A, Mougel V, et al. Surface organometallic and coordination chemistry toward single-site heterogeneous catalysts: strategies, methods, structures, and activities. Chem Rev 2016;116:323–421. https://doi.org/10.1021/acs.chemrev.5b00373.
[131] Ayodele OB. Influence of oxalate ligand functionalization on Co/ZSM-5 activity in Fischer Tropsch synthesis and hydrodeoxygenation of oleic acid into hydrocarbon fuels. Sci Rep 2017;7:1–14. https://doi.org/10.1038/s41598-017-09706-z.
[132] Ayodele OB, Lethesh KC, Gholami Z, Uemura Y. Effect of ethanedioic acid functionalization on Ni/Al_2O_3 catalytic hydrodeoxygenation and isomerization of octadec-9-enoic acid into biofuel: kinetics and Arrhenius parameters. J Energy Chem 2016;25:158–68. https://doi.org/10.1016/j.jechem.2015.08.017.
[133] Gamba O, Moreno S, Molina R. Catalytic performance of Ni-Pr supported on delaminated clay in the dry reforming of methane. Int J Hydrogen Energy 2011;36:1540–50. https://doi.org/10.1016/j.ijhydene.2010.10.096.
[134] Zhang S, Wang J, Wang X. Effect of calcination temperature on structure and performance of Ni/TiO_2-SiO_2 catalyst for CO_2 reforming of methane. J Nat Gas Chem 2008;17:179–83. https://doi.org/10.1016/S1003-9953(08)60048-1.
[135] Liu BS, Au CT. Carbon deposition and catalyst stability over La_2NiO_4/γ-Al_2O_3 during CO_2 reforming of methane to syngas. Appl Catal Gen 2003;244:181–95. https://doi.org/10.1016/S0926-860X(02)00591-4.
[136] Feng J, Ding Y, Guo Y, Li X, Li W. Calcination temperature effect on the adsorption and hydrogenated dissociation of CO_2 over the NiO/MgO catalyst. Fuel 2013;109:110–5. https://doi.org/10.1016/j.fuel.2012.08.028.
[137] Baraka S, Bouearan K, Caner L, Fontaine C, Epron F, Brahmi R, et al. Catalytic performances of natural Ni-bearing clay minerals for production of syngas from dry reforming of methane. J CO_2 Util 2021;52:101696. https://doi.org/10.1016/j.jcou.2021.101696.
[138] Liu H, Yao L, Hadj Taief HB, Benzina M, Da Costa P, Gálvez ME. Natural clay-based Ni-catalysts for dry reforming of methane at moderate temperatures. Catal Today 2018;306:51–7. https://doi.org/10.1016/j.cattod.2016.12.017.
[139] Fan MS, Abdullah AZ, Bhatia S. Utilization of greenhouse gases through carbon dioxide reforming of methane over Ni-Co/MgO-ZrO_2: preparation, characterization and activity studies. Appl Catal B Environ 2010;100:365–77. https://doi.org/10.1016/j.apcatb.2010.08.013.
[140] Nagaraja BM, Bulushev DA, Beloshapkin S, Ross JRH. The effect of potassium on the activity and stability of Ni-MgO-ZrO_2 catalysts for the dry reforming of methane to give synthesis gas. Catal Today 2011;178:132–6. https://doi.org/10.1016/j.cattod.2011.08.040.
[141] Koike M, Ishikawa C, Li D, Wang L, Nakagawa Y, Tomishige K. Catalytic performance of manganese-promoted nickel catalysts for the steam reforming of tar from biomass pyrolysis to synthesis gas. Fuel 2013;103:122–9. https://doi.org/10.1016/j.fuel.2011.04.009.
[142] Liu H, Da Costa P, Hadj Taief HB, Benzina M, Gálvez ME. Ceria and zirconia modified natural clay based nickel catalysts for dry reforming of methane. Int J Hydrogen Energy 2017;42:23508–16. https://doi.org/10.1016/j.ijhydene.2017.01.075.
[143] Daza CE, Gamba OA, Hernández Y, Centeno MA, Mondragón F, Moreno S, et al. High-stable mesoporous Ni-Ce/clay catalysts for syngas production. Catal Lett 2011;141:1037–46. https://doi.org/10.1007/s10562-011-0579-1.
[144] Wang S, Zhu HY, Lu GQ. Preparation, characterization, and catalytic properties of clay-based nickel catalysts for methane reforming. J Colloid Interface Sci 1998;204:128–34. https://doi.org/10.1006/jcis.1998.5553.
[145] Hwang KS, Zhu HY, Lu GQ. New nickel catalysts supported on highly porous alumina intercalated laponite for methane reforming with CO_2. Catal Today 2001;68:183–90. https://doi.org/10.1016/S0920-5861(01)00299-1.
[146] Sivaiah MV, Petit S, Barrault J, Batiot-Dupeyrat C, Valange S. CO_2 reforming of CH4 over Ni-containing phyllosilicates as catalyst precursors. Catal Today 2010;157:397–403. https://doi.org/10.1016/j.cattod.2010.04.042.
[147] Lu M, Fang J, Han L, Faungnawakij K, Li H, Cai S, et al. Coke-resistant defect-confined Ni-based nanosheet-like catalysts derived from halloysites for CO_2 reforming of methane. Nanoscale 2018;10:10528–37. https://doi.org/10.1039/c8nr02006j.
[148] Saravanan A, Kumar PS, Dai-Viet NVo, Jeevanantham S, Bhuvaneswari V, Narayanan VA, Yaashikaa PR, Swetha S, Reshma B. A comprehensive review on different approaches for CO_2 utilization and conversion pathways. Chem Eng Sci 2021;236:116515. https://doi.org/10.1016/j.ces.2021.116515.
[149] Lu Y, Guo D, Ruan Y, Zhao Y, Wang S, Ma X. Facile one-pot synthesis of Ni@HSS as a novel yolk-shell structure catalyst for dry reforming of methane. J CO_2 Util 2018;24:190–9. https://doi.org/10.1016/j.jcou.2018.01.003.
[150] Almana N, Phivilay SP, Laveille P, Hedhili MN, Fornasiero P, Takanabe K, et al. Design of a core–shell Pt–SiO_2 catalyst in a reverse microemulsion system: distinctive kinetics on CO oxidation at low temperature. J Catal 2016;340:368–75. https://doi.org/10.1016/j.jcat.2016.06.002.
[151] Li Z, Mo L, Kathiraser Y, Kawi S. Yolk-satellite-shell structured Ni-Yolk@Ni@SiO_2 nanocomposite: superb catalyst toward methane CO_2 reforming reaction. ACS Catal 2014;4:1526–36. https://doi.org/10.1021/cs401027p.
[152] Zhang J, Li F. Applied Catalysis B : environmental Coke-resistant Ni@SiO_2 catalyst for dry reforming of methane.

Appl Catal B Environ 2015;176–177:513–21. https://doi.org/10.1016/j.apcatb.2015.04.039.
[153] Polshettiwar V, Cha D, Zhang X, Basset JM. High-surface-area silica nanospheres (KCC-1) with a fibrous morphology. Angew Chem Int Ed 2010;49:9652–6. https://doi.org/10.1002/anie.201003451.
[154] Bayal N, Singh B, Singh R, Polshettiwar V. Size and fiber density controlled synthesis of fibrous nanosilica spheres (KCC-1). Sci Rep 2016;6:1–11. https://doi.org/10.1038/srep24888.
[155] Febriyanti E, Suendo V, Mukti RR, Prasetyo A, Arifin AF, Akbar MA, et al. Further insight on the definite morphology and formation mechanism of mesoporous silica KCC-1 some of them contradict with chemistry principles. 2016. https://doi.org/10.1021/acs.langmuir.6b00675.
[156] Kumar H, Sarma AK, Kumar P. A comprehensive review on preparation, characterization, and combustion characteristics of microemulsion based hybrid biofuels. Renew Sustain Energy Rev 2020;117:109498. https://doi.org/10.1016/j.rser.2019.109498.
[157] Maity A, Polshettiwar V. Dendritic fibrous nanosilica for catalysis, energy harvesting, carbon dioxide mitigation, drug delivery, and sensing. ChemSusChem 2017;10:3866–913. https://doi.org/10.1002/cssc.201701076.
[158] Lee S, Shantz DF. Zeolite growth in nonionic microemulsions: synthesis of hierarchically structured zeolite particles. Chem Mater 2005;17:409–17. https://doi.org/10.1021/cm0486114.
[159] Teh LP, Setiabudi HD, Timmiati SN, Aziz MAA, Annuar NHR, Ruslan NN. Recent progress in ceria-based catalysts for the dry reforming of methane: a review. Chem Eng Sci 2021;242:116606. https://doi.org/10.1016/j.ces.2021.116606.
[160] Fatah NAA, Jalil AA, Rahman AFA, Hambali HU, Hussain I. CO_2 methanation over mesoporous silica based catalyst: a comprehensive study. J Energy Saf Technol 2019;2:49–53. https://doi.org/10.11113/jest.v2n2.51.
[161] Hussain I, Jalil AA, Hassan NS, Hamid MYS. Recent advances in catalytic systems for CO_2 conversion to substitute natural gas (SNG): perspective and challenges. J Energy Chem 2021;62:377–407. https://doi.org/10.1016/j.jechem.2021.03.040.
[162] Bukhari SN, Chong CC, Setiabudi HD, Cheng YW, Teh LP, Jalil AA. Ni/Fibrous type SBA-15: highly active and coke resistant catalyst for CO_2 methanation. Chem Eng Sci 2021;229:116141. https://doi.org/10.1016/j.ces.2020.116141.
[163] Azami MS, Jalil AA, Hitam CNC, Mamat CR, Siang TJ, Hussain I, et al. A contemporary assessment on composite titania onto graphitic carbon nitride-based catalyst as photocatalyst. J Energy Saf Technol 2019;2:21–5. https://doi.org/10.11113/jest.v2n1.39.
[164] Azami MS, Jalil AA, Hitam CNC, Hassan NS, Mamat CR, Adnan RH, et al. Tuning of the electronic band structure of fibrous silica titania with g-C_3N_4 for efficient Z-scheme photocatalytic activity. Appl Surf Sci 2020;512:145744. https://doi.org/10.1016/j.apsusc.2020.145744.
[165] Aziz FFA, Jalil AA, Hassan NS, Fauzi AA, Azami MS. Simultaneous photocatalytic reduction of hexavalent chromium and oxidation of p-cresol over AgO decorated on fibrous silica zirconia. Environ Pollut 2021;285:117490. https://doi.org/10.1016/j.envpol.2021.117490.
[166] Fauzi AA, Jalil AA, Hitam CNC, Aziz FFA, Chanlek N. Superior sulfate radicals-induced visible-light-driven photodegradation of pharmaceuticals by appropriate Ce loading on fibrous silica ceria. J Environ Chem Eng 2020;8:104484. https://doi.org/10.1016/j.jece.2020.104484.
[167] Ibrahim M, Jalil AA, Khusnun NF, Fatah NAA, Hamid MYS, Gambo Y, et al. Enhanced n-hexane hydroisomerization over bicontinuous lamellar silica mordenite supported platinum (Pt/HM@KCC-1) catalyst. Int J Hydrogen Energy 2020;45:18587–99. https://doi.org/10.1016/j.ijhydene.2019.04.067.
[168] Maity A, Belgamwar R, Polshettiwar V. Facile synthesis to tune size, textural properties and fiber density of dendritic fibrous nanosilica for applications in catalysis and CO_2 capture. Nat Protoc 2019;14:2177–204. https://doi.org/10.1038/s41596-019-0177-z.
[169] Siang TJ, Jalil AA, Abdulrasheed AA, Hambali HU, Nabgan W. Thermodynamic equilibrium study of altering methane partial oxidation for Fischer–Tropsch synfuel production. Energy 2020. https://doi.org/10.1016/j.energy.2020.117394.
[170] Osarieme UO, Sumaiya ZA. An overview on the role of lanthanide series (rare earth metals) in H_2 and syngas production from CH_4 reforming processes. Chem Eng Sci 2020;227:115863. https://doi.org/10.1016/j.ces.2020.115863.
[171] Izhab I, Asmadi M, Saidina Amin NA. Methane dry reforming using oil palm shell activated carbon supported cobalt catalyst: multi-response optimization. Int J Hydrogen Energy 2021;46:24754–67. https://doi.org/10.1016/j.ijhydene.2020.04.188.
[172] Nyakuma BB, Wong SL, Faizal HM, Hambali HU, Oladokun O, Abdullah TAT. Carbon dioxide torrefaction of oil palm empty fruit bunches pellets: characterisation and optimisation by response surface methodology. Biomass Convers Biorefinery 2020. https://doi.org/10.1007/s13399-020-01071-8.
[173] Izhab I, Asmadi M, Saidina Amin NA. Methane dry reforming using oil palm shell activated carbon supported cobalt catalyst: multi-response optimization. Int J Hydrogen Energy 2020. https://doi.org/10.1016/j.ijhydene.2020.04.188.
[174] Sidik SM, Triwahyono S, Jalil AA, Aziz MAA, Fatah NAA, Teh LP. Tailoring the properties of electrolyzed Ni/mesostructured silica nanoparticles (MSN) via different Ni-loading methods for CO_2 reforming of CH_4. J CO_2 Util 2016;13:71–80. https://doi.org/10.1016/j.jcou.2015.12.004.
[175] Liu D, Quek XY, Cheo WNE, Lau R, Borgna A, Yang Y. MCM-41 supported nickel-based bimetallic catalysts with superior stability during carbon dioxide reforming of methane: effect of strong metal-support interaction. J Catal 2009;266:380–90. https://doi.org/10.1016/j.jcat.2009.07.004.
[176] Alotaibi R, Alenazey F, Alotaibi F, Wei N, Al-fatesh Ahmed, Fakeeha A. Ni Catalysts with different promoters supported on zeolite for dry reforming of methane. Appl Petrochem Res 2015;5:329–37. https://doi.org/10.1007/s13203-015-0117-y.
[177] Fakeeha AH, Khan WU, Al-Fatesh AS, Abasaeed AE. Stabilities of zeolite-supported Ni catalysts for dry reforming of methane. Cuihua Xuebao/Chinese J Catal 2013;34:764–8. https://doi.org/10.1016/s1872-2067(12)60554-3.
[178] De Jesus AS, Malcony ML, Batista MS. Effect of MgO loading over zeolite-supported Ni catalysts in methane reforming with carbon dioxide for synthesis gas production. React Kinet Mech Catal 2017;122:501–11. https://doi.org/10.1007/s11144-017-1218-7.
[179] Najfach AJ, Almquist CB, Edelmann RE. Effect of manganese and zeolite-supported Ni-catalysts for dry reforming of methane. Catal Today 2020. https://doi.org/10.1016/j.cattod.2020.07.058.
[180] Moradi G, Khezeli F, Hemmati H. Syngas production with dry reforming of methane over Ni/ZSM-5 catalysts. J Nat Gas Sci Eng 2016;33:657–65. https://doi.org/10.1016/j.jngse.2016.06.004.
[181] Frontera P, Macario A, Aloise A, Crea F, Antonucci PL, Nagy JB, et al. Catalytic dry-reforming on Ni – zeolite

supported catalyst. Catal Today 2012;179:52–60. https://doi.org/10.1016/j.cattod.2011.07.039.
[182] Drobná H, Kout M, Sołtysek A, González-Delacruz VM, Caballero A, Čapek L. Analysis of Ni species formed on zeolites, mesoporous silica and alumina supports and their catalytic behavior in the dry reforming of methane. React Kinet Mech Catal 2017;121:255–74. https://doi.org/10.1007/s11144-017-1149-3.
[183] Kaengsilalai A, Luengnaruemitchai A, Jitkarnka S, Wongkasemjit S. Potential of Ni supported on KH zeolite catalysts for carbon dioxide reforming of methane. J Power Sources 2007;165:347–52. https://doi.org/10.1016/j.jpowsour.2006.12.005.
[184] Ayodele BV, Cheng CK. Modelling and optimization of syngas production from methane dry reforming over ceria-supported cobalt catalyst using artificial neural networks and Box-Behnken design. J Ind Eng Chem 2015;32:246–58. https://doi.org/10.1016/j.jiec.2015.08.021.
[185] Nataj SMM, Alavi SM, Mazloom G. Modeling and optimization of methane dry reforming over Ni–Cu/Al_2O_3 catalyst using Box–Behnken design, vol. 27. Elsevier B.V.; 2018. https://doi.org/10.1016/j.jechem.2017.10.002.
[186] Rosha P, Singh R, Mohapatra SK, Mahla SK, Dhir A. Optimization of hydrogen-enriched biogas by dry oxidative reforming with nickel nanopowder using response surface methodology. Energy Fuel 2018;32:6995–7001. https://doi.org/10.1021/acs.energyfuels.8b00819.
[187] Marmarshahi S, Niaei A, Salari D, Abedini F, Abbasi M, Kalantari N. Evaluating the catalytic performance of $La_{1-x}Ce_xNi_{1-y}Zn_yO_3$ nanostructure perovskites in the carbon dioxide reforming of methane. Procedia Mater Sci 2015;11:616–21. https://doi.org/10.1016/j.mspro.2015.11.095.
[188] Sidik SM, Triwahyono S, Jalil AA, Majid ZA, Salamun N, Talib NB, Abdullah TAT. CO_2 reforming of CH_4 over Ni–Co/MSN for syngas production: role of Co as a binder and optimization using RSM. Chem Eng J 2016;295:1–10. https://doi.org/10.1016/j.cej.2016.03.041.
[189] Braga TP, Santos RCR, Sales BMC, da Silva BR, Pinheiro AN, Leite ER, et al. CO_2 mitigation by carbon nanotube formation during dry reforming of methane analyzed by factorial design combined with response surface methodology. Cuihua Xuebao/Chinese J Catal 2014;35:514–23. https://doi.org/10.1016/s1872-2067(14)60018-8.
[190] Fan MS, Abdullah AZ, Bhatia S. Hydrogen production from carbon dioxide reforming of methane over Ni-Co/MgO-ZrO_2 catalyst: process optimization. Int J Hydrogen Energy 2011;36:4875–86. https://doi.org/10.1016/j.ijhydene.2011.01.064.
[191] Medeiros RLBA, Macedo HP, Melo VRM, Oliveira ÂAS, Barros JMF, Melo MAF, et al. Ni supported on Fe-doped $MgAl_2O_4$ for dry reforming of methane: use of factorial design to optimize H2 yield. Int J Hydrogen Energy 2016;41:14047–57. https://doi.org/10.1016/j.ijhydene.2016.06.246.
[192] Ayodele BV, Khan MR, Nooruddin SS, Cheng CK. Modelling and optimization of syngas production by methane dry reforming over samarium oxide supported cobalt catalyst: response surface methodology and artificial neural networks approach. Clean Technol Environ Policy 2017;19:1181–93. https://doi.org/10.1007/s10098-016-1318-5.
[193] Abbasi M, Niaei A, Salari D, Hosseini SA, Abedini F, Marmarshahi S. Modeling and optimization of synthesis parameters in nanostructure La1–xBaxNi1–yCuyO3 catalysts used in the reforming of methane with CO_2. J Taiwan Inst Chem Eng 2017;74:187–95. https://doi.org/10.1016/j.jtice.2017.02.013.
[194] Mei DH, Liu SY, Tu X. CO_2 reforming with methane for syngas production using a dielectric barrier discharge plasma coupled with Ni/γ-Al_2O_3 catalysts: process optimization through response surface methodology. J CO_2 Util 2017;21:314–26. https://doi.org/10.1016/j.jcou.2017.06.020.
[195] Li Z, Lin Q, Li M, Cao J, Liu F, Pan H, Wang Z, Kawi S. Recent advances in process and catalyst for CO2 reforming of methane. Renew Sustain Energy Rev 2020;134:110312. https://doi.org/10.1016/j.rser.2020.110312.
[196] Mohammed AK, Idem R, Saha B. Sulfur tolerant catalysts for hydrogen production by carbon dioxide reforming of methane-rich gas. U.S. Patent US009339797B2; 2016.
[197] Chun YN. Microwave reforming apparatus for gas reforming. U.S.: Industry academci cooperation foundation chosun university; 2019.
[198] Akira TNM, Nakamura T. Process for reforming hydrocarbons with carbon dioxide by the use of a selectivity permeable membrane reactor. U.S.: NGK Insulators, Ltd.; 2008.
[199] Hanson DC, Stal JA. The first commercial sulphur passivated reforming (SPARG) plant, Topsoe Seminar on Synthesis Gas Technologies. Google Scholar, https://scholar.google.com/scholar?q=The%20first%20commercial%20sulphur%20passivated%20reforming%20%20plant; 1990.
[200] CT ST, Neumann P, Von Linde F. The calcor standard and calcor economy processes. Oil Gas Eur Mag 2001;45.
[201] Green Car Congress. Carbon Science licenses catalyst technology for carbon dioxide reforming of methane from University of Saskatchewan. Green Car Congress; 2010. https://www.greencarcongress.com/2010/12/csi-20101228.html.
[202] Group TL. Innovative dry reforming process successful catalyst upscaling. https://www.linde-engineering.com/en/innovations/innovate-dry-reforming/index.html.
[203] Das S, Jangam A, Xi S, Borgna A, Hidajat K, Kawi S. Highly dispersed Ni/silica by carbonization-calcination of a chelated precursor for coke-free dry reforming of methane. ACS Appl Energy Mater 2020;3:7719–35. https://doi.org/10.1021/acsaem.0c01122.
[204] Li S, Fu Y, Kong W, Pan B, Yuan C, Cai F, Zhu H, Zhang J, Sun Y. Dually confined Ni nanoparticles by room-temperature degradation of AlN for dry reforming of methane. Appl Catal B Environ 2020;277. https://doi.org/10.1016/j.apcatb.2020.118921.
[205] Yang B, Deng J, Li H, Yan T, Zhang J, Zhang D. Coking-resistant dry reforming of methane over Ni/γ-Al_2O_3 catalysts by rationally steering metal-support interaction. iScience 2021;24:102747. https://doi.org/10.1016/j.isci.2021.102747.
[206] Li M, Veen ACV. Tuning the catalytic performance of Ni-catalysed dry reforming of methane and carbon deposition via Ni-CeO_{2-x} interaction. Appl Catal B Environ 2018;237:641–8. https://doi.org/10.1016/j.apcatb.2018.06.032.
[207] Ma Q, Han Y, Wei Q, Makpal S, Gao X, Zhang J, Zhao TS. Stabilizing Ni on bimodal mesoporous-macroporous alumina with enhanced coke tolerance in dry reforming of methane to syngas. J CO_2 Util 2020;35:288–97. https://doi.org/10.1016/j.jcou.2019.10.010.
[208] Li B, Yuan X, Li B, Wang X. Ceria-modified nickel supported on porous silica as highly active and stable catalyst for dry reforming of methane. Fuel 2021;301:121027. https://doi.org/10.1016/j.fuel.2021.121027.
[209] Li K, Chang X, Pei C, Li X, Chen S, Zhang X, Assabumrungrat S, Zhao ZJ, Zeng L, Gong J. Ordered

mesoporous Ni/La_2O_3 catalysts with interfacial synergism towards CO_2 activation in dry reforming of methane. Appl Catal B Environ 2019;259:118092. https://doi.org/10.1016/j.apcatb.2019.118092.

[210] Wan C, Song K, Pan J, Huang M, Luo R, Li D, Jiang L. Ni–Fe/Mg(Al)O alloy catalyst for carbon dioxide reforming of methane: influence of reduction temperature and Ni–Fe alloying on coking. Int J Hydrogen Energy 2020;45:33574–85. https://doi.org/10.1016/j.ijhydene.2020.09.129.

[211] Shah S, Sayono S, Ynzunza J, Pan R, Xu M, Pan X, Gilliard-AbdulAziz KL. The effects of stoichiometry on the properties of exsolved Ni-Fe alloy nanoparticles for dry methane reforming. AIChE J 2020;66:1–12. https://doi.org/10.1002/aic.17078.

[212] Zhang T, Liu Z, Zhu YA, Liu Z, Sui Z, Zhu K, Zhou X. Dry reforming of methane on Ni-Fe-MgO catalysts: influence of Fe on carbon-resistant property and kinetics. Appl Catal B Environ 2020;264:118497. https://doi.org/10.1016/j.apcatb.2019.118497.

[213] Jin F, Fu Y, Kong W, Wang J, Cai F, Yuan C, Pan B, Zhang J, Sun Y. Stable trimetallic NiFeCu catalysts with high carbon resistance for dry reforming of methane. Chempluschem 2020;85:1120–8. https://doi.org/10.1002/cplu.202000217.

[214] Shah S, Xu M, Pan X, Gilliard-Abdulaziz KL. Exsolution of embedded Ni-Fe-Co nanoparticles: implications for dry reforming of methane. ACS Appl Nano Mater 2021;4:8626–36. https://doi.org/10.1021/acsanm.1c02268.

[215] De Coster V, Srinath NV, Theofanidis SA, Pirro L, Van Alboom A, Poelman H, Sabbe MK, Marin GB, Galvita VV. Looking inside a Ni-Fe/$MgAl_2O_4$ catalyst for methane dry reforming via Mössbauer spectroscopy and in situ QXAS. Appl Catal B Environ 2022;300. https://doi.org/10.1016/j.apcatb.2021.120720.

[216] Theofanidis SA, Galvita VV, Poelman H, Marin GB. Enhanced carbon-resistant dry reforming Fe-Ni catalyst: role of Fe. ACS Catal 2015;5:3028–39. https://doi.org/10.1021/acscatal.5b00357.